The Astrophysical Journal, 891:128 (18pp), 2020 March 10 https://doi.org/10.3847/1538-4357/ab6ffa

A Transition of Dynamo Modes in M Dwarfs: Narrowing Down the Spectral Range Where the Transition Occurs*

D. J. Mullan[1] and E. R. Houdebine[2,3]
[1] Dept. of Physics and Astronomy, University of Delaware, Newark, DE 19716, USA
[2] Armagh Observatory, College Hill, BT61 9DG Armagh, UK
[3] Université Paul Sabatier, Observatoire Midi-Pyrénées, CNRS, CNES, IRAP, F-31400 Toulouse, France
Received 2019 October 11; revised 2020 January 20; accepted 2020 January 22; published 2020 March 12

Abstract

Houdebine et al. combined Ca II data with projected rotational velocities (v sin i) to construct rotation-activity correlations (RAC) in K-M dwarfs. The RAC slopes were used to argue that a transition between dynamo modes occurs at a spectral type between M2 and M3. H17 suggested that the dynamo transition corresponds to a transition to complete convection (TTCC). An independent study of *GAIA* data led Jao et al. to suggest that the TTCC sets in "near M3.0V," close to the H17 result. However, the changes in a star that cause TTCC signatures in *GAIA* data might not lead to changes in Ca II emission at an identical spectral type: the latter are also affected by magnetic effects, which depend on certain properties of convection in the core. Here, we use Ca II emission fluxes in a sample of ∼600 M dwarfs, and attempt to narrow down the transition from one dynamo mode to another: rather than relying on RAC slopes, we quantify how the Ca II emission flux varies with spectral type to identify "steps" where the flux decreases significantly across a narrow range of spectral types. We suggest that the dynamo mode transition may be narrowed down to between M2.1 and M2.3. This is close to, but earlier than, the TTCC location identified by Jao et al. We suggest that the transition in dynamo mode may be related to the existence of a small convective core, which occurs for a finite time interval in certain low-mass stars.

Unified Astronomy Thesaurus concepts: Astrophysical processes (104); Stellar chromospheres (230)

1. Introduction

Houdebine et al. (2017; hereafter referred to as H17) reported on measurements of the fluxes of chromospheric emission in the Ca II lines in a sample of (272) lower main-sequence stars with spectral subtypes of K4, K6, M2, M3, and M4. Using archival spectra which had been obtained over many years by the HARPS and SOPHIE spectrometers, the flux F(Ca II) of the Ca II emission in each star was extracted.

It is important to clarify how, in the present paper, we define "the" flux F(Ca II) for each star in our sample. It is known that chromospheres in stars are variable on timescales that range from as short as days (rotational modulation) to as long as years (activity cycles?; e.g., Suarez Mascareno et al. 2016). The spectra we analyze in the present paper were derived from archival data that were gathered originally in connection with planet-search programs using the SOPHIE, HARPS, and FEROS instruments. These observations, designed to search for small variations in radial velocity associated with reflex motion of the star as a planet orbits, are distributed over a span of many years. As a result, the archival data include many spectra for each star, distributed randomly in time. Typically, each star in our sample has dozens of spectra: many have 100 or more, and the limiting case is more than 700 for Prox Cen. Stars that were observed a few times only are in the minority. Therefore, when we report "the" F(Ca II) for any particular star, the numerical value is an average over multiple random epochs. The averaging process smooths out any variations due to rotation and/or activity cycles.

An anonymous referee has raised the issue of possible misclassifications of active/inactive stars due to variability. In order to avoid such difficulties, we have excluded from our statistics the subdwarfs and the intermediate dM(e) stars, which have peculiar metal abundances and/or spectral properties. Only normal low- and high-activity dwarfs are included in our samples.

As a result of these precautions, our measured EWs can be considered as representative averages of "the" Ca II emission flux for each star.

1.1. Chromospheric Heating and Dynamo Operation

The flux of Ca II emission from a star is a (partial) measure of how effective the chromospheric heating is in that star. In any star, mechanical work of some kind is required to heat the chromosphere to temperatures that exceed the photospheric value: the transport of heat inside the star that leads to a temperature that declines with increasing radial location is a natural feature of radiative and convective transfer of energy outward. But the onset of increasing local temperatures above a certain height requires the presence of an agent (or agents) that performs work on the local material in order to raise the temperature a few thousands of degrees above that predicted by radiative equilibrium (e.g., Mullan 2009). Agents that perform such work include acoustic waves and also magnetic fields. All low-mass stars possess deep convective envelopes where acoustic waves are inevitably generated by the ubiquitous pressure fluctuations that are inevitable in a compressible medium: as a result, acoustically heated chromospheres are present in all low-mass stars. But stars can also generate chromospheres by means of heating due to magnetic processes, including dissipation of MHD waves of various kinds (Alfvenic, slow MHD, fast MHD; e.g., Osterbrock 1961),

* Based in part on observations made at l'Observatoire de Haute Provence (CNRS) and at Pic-du-Midi Observatory, France. Also based on data obtained from the SOPHIE archive (OHP) and from the FEROS, HARPS, and UVES archives (European Southern Observatory).

dissipation of electric currents (e.g., Goodman 1995), and nanoflares (e.g., Jess et al. 2014). Naturally, the magnetic mechanisms require the presence of magnetic fields in the star. Schrijver (1983) suggested that at any given spectral type, stars with the weakest chromospheric emissions might be regarded as representatives of the lowest permissible heating: the term "basal flux" was coined to refer to the lower limit on mechanical energy flux in a star of any particular spectral type. It is widely believed that the chromosphere in such stars is acoustically heated. Stars with chromospheric emissions that exceed the basal fluxes are considered to contain sources of both acoustic plus magnetic heating. In the present paper, we are interested in stars where the chromospheres lie close to the basal flux, but which also include at least some magnetic contributions.

Regarding the magnetic contributions, dynamos of three major kinds have been modeled in the literature (e.g., Racine et al. 2011): these are referred to by the labels $\alpha\Omega$, α^2, and $\alpha^2\,\Omega$. In these labels, the parameter α quantifies a physical process (kinetic helicity), which, by means of local motions of the gas, creates an electric field that is related to the strength of the mean magnetic field. Parker (1955) suggested that the "α-effect" could occur in convective turbulence if cyclonic motions (driven by rotation) were available to systematically deflect and twist the stellar magnetic field. Also in the above labels, Ω is the angular velocity: more formally, the important physical parameter in the dynamo operation is not so much the absolute magnitude of Ω but rather the radial *gradient* of Ω.

It is important, in the context of the present paper, to note that some of the stars in our sample are sufficiently massive that they contain an interface between a radiative core and a convective envelope inside the star. At such an interface, physical conditions may lead to a steep local radial gradient of Ω inside a thin turbulent boundary layer: this layer (the tachocline) is expected to be the site of effective dynamo activity (e.g., Spiegel & Zahn 1992). In fact, with regards to dynamo activity in our own Sun, the argument can be made that the site of solar activity in fact lies in a layer *near the lower edge* of the tachocline (Stenflo 1991). Stars on the lower main sequence are expected to have convective envelopes that may be considerably deeper than the zone in the Sun (Stromgren 1952; Osterbrock 1953): in limiting cases, the convection zone may extend all the way to the center of the star. Based on theoretical work by Limber (1958), who computed the first fully convective models of M dwarfs, it is expected that in some of the stars in our sample, a tachocline is indeed present, whereas in other stars in our sample, there is no such interface. In the latter case, the star is completely convective. According to a particular model of stellar structure, the transition to complete convection (TTCC) is predicted to occur among main-sequence stars with masses in the range 0.32–0.34 $M_{\odot}$ (Mullan et al. 2015).

It is important to note that the overall sensitivity to rotation varies from one kind of dynamo process to another. These variations play an essential role in the interpretation we place on chromospheric heating in low-mass stars.

Observational evidence based on Zeeman–Doppler imaging of low-mass stars indicates that certain differences can be identified between the magnetic field properties in stars above and below the TTCC. Exempli gratia, the surface fields tend to be stronger in certain fully convective stars than in stars with a radiative core, although weak fields can also be present on other fully convective stars (Morin 2012). Moreover, completely convective stars generate fields that are predominantly poloidal, whereas in stars above the TTCC (i.e., stars with radiative cores), the fields are predominantly toroidal (See et al. 2016). Our goal is to determine if any observational signature can be identified in Ca II emission data associated with the TTCC.

The plan of the paper is as follows. In Section 1.2, we describe how the rotational sensitivity of Ca II emission in K and M dwarfs can be quantified: specifically, we examine the empirical rotation-activity correlation (RAC), and extract numerical values for the *slope* of the RAC. The results that emerged (in H17) from our use of the RAC slope technique are summarized in Section 1.3. Our interpretation of these results in terms of dynamo models are summarized in Section 1.4, where we recapitulate the major conclusion of H17: something interesting happens in the Ca II emission properties of stars with spectral types between M2 and M3, perhaps indicating a change in the dynamo mode. In Section 1.5, we raise the question: can more than one dynamo mechanism be at work in a given star? In Section 1.6, we summarize a completely independent study (using *GAIA* data), which, more than a year after the H17 paper appeared, reported that the stellar luminosity function exhibits an empirical feature "near spectral type M3.0V." We summarize theoretical work that attributes the empirical feature to the onset of complete convection and discuss how this result provides independent support for the major conclusion of H17. In Section 1.7, we turn to consider the information that was contained in our earlier paper (H17) regarding the *absolute levels* of the fluxes of chromospheric emission in Ca II as a function of spectral type. The main purpose of the present paper is to extend the H17 data set with new data on Ca II emission (in terms of equivalent widths and absolute fluxes) in a larger sample of stars. These new data are presented in Section 2, where we show (in Figures 3–5) how the Ca II emission flux declines as we go toward later spectral subtypes among inactive and active M dwarfs. In Section 3, our Ca II empirical emission fluxes in inactive M dwarfs are compared with theoretical predictions that have been made by Ulmschneider et al. (1996) for the acoustic power generation in cool dwarfs. In Section 4, we raise the issue: Does any significant "feature" exist in the curve of Ca II emission fluxes versus spectral type? We discuss if such a "feature" might be associated with a change in dynamo behavior when a low-mass main-sequence star becomes completely convective. Conclusions are presented in Section 5.

1.2. Distinguishing between Different Processes of Chromospheric Heating: the RAC Slope Technique

Is there a way to distinguish between a chromosphere in a star where one form of heating dominates from the chromosphere of another star in which another heating mechanism dominates? One possibility is to examine the rotation of the star: dynamos are expected to rely to a greater or lesser extent on rotational motion in order to operate, whereas acoustic fluxes are not expected to be sensitive to rotation. Thus, if we can identify an empirical relationship between rotation and magnetic activity (the latter being quantified by the strength of chromospheric emission), separation of one form of heating from another might be possible. This applies not merely to distinguishing acoustic heating from magnetic heating: we

might also hope to distinguish one type of magnetic heating from another.

In H17, the fluxes of emission in the chromospheric lines of Ca II were obtained from archival spectra. But also from the same spectra, rotational information ($v \sin i$) was obtained by cross-correlating the profiles of hundreds of photospheric lines. By plotting F(Ca II) emission fluxes versus the (projected) rotational period $P/\sin i$ for our sample of stars in each spectral subtype, an RAC was derived for each of the five spectral subtypes. For stars in each spectral subtype, in a plot of the RAC, i.e., in a plot of log[F(Ca II)] versus log[$P/\sin i$], least-squares fitting was used to determine a value for the slope of the best-fitting line. In all cases, the slope was found to have a negative value, i.e., the faster a star rotates, the stronger the chromospheric emission in Ca II is. The chromospheric emission is sensitive to rotation.

The absolute magnitude of the slope that is associated with the RAC at any particular spectral subtype is a measure of how sensitive the chromospheric emission is to rotation for stars of that spectral subtype. For stars of some spectral subtypes, the slope is found to have a large absolute magnitude: for such stars, we say that the RAC has a *steep* slope. If a steep RAC slope is discovered in any sample of stars, this suggests the operation of a dynamo in which rotation plays a dominant role. In such stars, it is believed that there is a dynamo at work such that faster rotation generates significantly stronger magnetic fields: in the presence of such stronger magnetic fields, stronger chromospheric heating is expected, thereby giving rise to more intense emission in, e.g., the Ca II lines. The dynamo in such stars, where rotational sensitivity is maximal, might be an interface dynamo, perhaps an $\alpha\Omega$ dynamo.

On the other hand, if a *shallow* RAC slope is discovered in a sample of stars, this suggests that rotation plays a less important role in the dynamo operation. An example of such a dynamo is an α^2 (or $\alpha^2\,\Omega$) dynamo, which relies on the existence of small-scale turbulent eddies distributed throughout the extensive convective envelope of a low-mass star. The dependence on eddies with a wide spatial distribution leads to terms such as "distributed dynamo" or "small-scale dynamo": in such a dynamo, rotation still contributes somewhat to the dynamo process, but the contribution is not as dominant as in an $\alpha\Omega$ dynamo (Durney et al. 1993). In what follows, we shall use the short-hand notation α^2 dynamo as a proxy for a distributed or small-scale dynamo in which the effects of rotation are relatively weak.

1.3. Comparison of RAC Slopes for Low-activity Stars and High-activity Stars

In H17, in order to perform a meaningful analysis of the Ca II fluxes, our attention was mainly focused on deriving the slope of the RAC at each spectral subtype. In preparation for this study, the overall sample of 272 stars was separated into sub-samples of "low-activity" (with no detectable Hα emission) and "high-activity" (with measurable emission in the Hα line). It was found that this separation of stars based on activity levels leads to a helpful ordering of the data.

In all points plotted in Figure 1, we plot (as a filled circle) the mean value of the RAC slope for a particular spectral subtype, as well as the 3σ standard deviation above and below the mean.

In the lower part of Figure 1, the plotted data refer to the RAC slopes that were obtained for the low-activity stars, i.e., those with spectral types dK and dM. For these stars, the slope

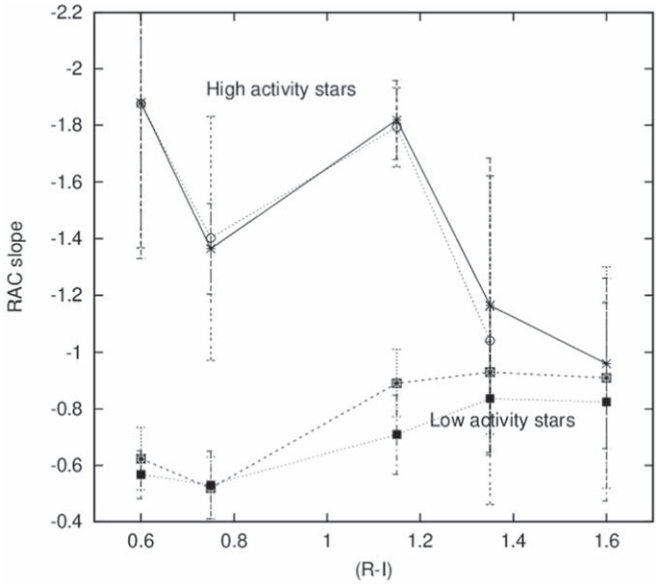

Figure 1. Numerical value of the slope of the rotation-activity correlation (RAC) for samples of stars belonging to different spectral subtypes. Each spectral sub-sample is characterized by its $(R-I)_C$ color (plotted along the abscissa in the above plot). For the stars in each spectral sub-sample, an RAC is constructed by means of a log–log plot of a chromospheric parameter (Ca II emission flux) vs. a rotational parameter ($P/\sin i$): then an RAC slope is determined by least-squares fitting. In the above figure, the RAC slope for each spectral sub-sample is plotted along the vertical axis. The lower curves refer to low-activity stars. The upper curves refer to high-activity stars. In both upper and lower curves, solid (dashed) lines refer to heteroscedastic (homoscedastic) least-squares fits to the data. Adapted from Houdebine et al. (2017, hereafter H17).

of the RAC was found to be *shallow* (−0.5 to −0.9). It is noteworthy that, for the low-activity stars in our sample, the slopes are found to be relatively shallow in all spectral subtypes that are included in our sample, i.e., ranging from dK4 to dM4. That is, for *all* low-activity stars in our sample, the values of the slopes, as plotted in Figure 1, remain closer to the horizontal axis than for any other sub-sample of our stars.

On the other hand, when we consider the high-activity stars, the slopes of the RAC were found to follow a more complicated pattern. When we consider the earliest subtypes of these stars, i.e., dK4e, dK6e, and dM2e, the slopes were found to be *steep* (−1.4 to −1.9): see the upper left part of Figure 1. In contrast, when we consider the two latest subtypes of high-activity stars (dM3e, dM4e), the slope was found to shift toward *shallower* values (−0.9 to −1.2): see lower right area of Figure 1.

Note on statistics: many of the spectra used in H17 were obtained partly from archives of the HARPS spectrograph, which was designed with a view to searching for exoplanets. Because of the small-amplitude velocity that would be induced by a planetary companion, the selection of target stars was planned in such a way as to exclude as many sources of noise as possible. One such source is activity on the star: the appearance and disappearance of temporary dark spots and bright plages distort the line profiles of the parent star, thereby obscuring the (small) shifts of the line that might be associated with the presence of a planet. As a result, the selection of target stars for the HARPS instrument was biased *in favor of* stars with low levels of activity, and biased *against* stars with the highest levels of chromospheric activity. The existence of this bias explains why, at, e.g., spectral type M2, the H17 sample

contained 54 low-activity stars (with spectral type dM2) while the number of high-activity stars (with spectral type dM2e) amounted to only 11. The bias that is present in HARPS data against high levels of activity should not be interpreted to mean that, in our study, we excluded active stars (i.e., those with spectral types dKe and dMe) entirely: on the contrary, the presence of a significant minority of active stars in our sample specifically enables us to contrast the chromospheric properties of stars where acoustic fluxes may dominate from those where magnetic processes may dominate. An anonymous referee has pointed out that an advantage of including both active and inactive stars in our sample is that "differences in chromospheric heating driven by different dynamo mechanisms may grow more obvious while possible uncertainties/variations in the basal flux level as a function of $T_{\rm eff}$ would be mitigated." In the present paper, we will present results for fluxes of Ca II emission in *both* active and inactive stars: the conclusions we will draw turn out to be similar for both groups.

Despite the relatively small samples of high-activity stars, it is important to note the statistical significance that is attached to the RAC slopes, which are plotted in Figure 1. This significance will allow us to quantify the differences that exist between the RAC slopes among active stars and the RAC slopes in inactive stars.

Specifically, referring to Table 1 in H17, the RAC slope for K4e stars (using homoscedastic least-squares fits) is found to have a value of -1.88 ± 0.55, while for the K4 stars, the RAC slope is -0.62 ± 0.11. Thus, at the 3σ level, our data indicate that the shallowest RAC slope for K4e stars (-1.33) is widely separated from the steepest RAC slope for K4 stars (-0.73): the separation between these extremes in slope is clearly in excess of 3σ.

Similarly, the RAC slope for K6e stars (using homoscedastic least-squares fits) is found to have a value of -1.36 ± 0.16, while for the K6 stars, the RAC slope is -0.52 ± 0.11. Thus, at the 3σ level, our data indicate that the shallowest RAC slope for K6e stars (-1.20) is widely separated from the steepest RAC slope for K6 stars (-0.63), i.e., a separation well in excess of 3σ. And if we examine the same parameters using heteroscedastic least-squares fits, we find that at the 3σ level, our data indicate that the shallowest RAC slope for K6e stars (-0.97) is widely separated from the steepest RAC slope for K6 stars (-0.65): the separation between these extremes in slope is again clearly in excess of 3σ.

Similarly, for M2e stars, the RAC slope (using homoscedastic fitting) is found to have a value of -1.82 ± 0.14, while for M2 stars, the RAC slope has a value of -0.89 ± 0.12. Thus, at the 3σ level, the shallowest RAC slope for M2e stars (-1.67) is widely separated from the steepest RAC slope for M2 stars (-1.01): the separation between these extremes in slope is once again clearly in excess of 3σ. A similar conclusion emerges from examination of the heteroscedastic least-squares fitting for M2 stars. Therefore, for the K6 and M2 stars in our sample, the RAC slopes of the high-activity stars are *steeper*, by a statistically significant amount ($>3\sigma$), than the RAC slopes of the low-activity stars.

However, a different statistical behavior emerges at spectral types M3 and M4. In both of these cases, Table 1 in H17 indicates that at the 3σ level, the RAC slopes *overlap*. (This conclusion is true in both homoscedastic or heteroscedastic fitting cases.) Exempli gratia, for M3e stars, the RAC slope is found to be -1.17 ± 0.52 while for M3 stars, the slope is found to be -0.93 ± 0.22. That is, in a statistical sense, the RAC slope for active M3e stars can *not* be distinguished from the RAC slope for inactive M3 stars. Likewise, for M4e and M4 stars, the RAC slopes are found to be -0.96 ± 0.30 and -0.91 ± 0.39, respectively: therefore, again in a statistical sense, the RAC slope for active M4e stars is indistinguishable from the RAC slope for inactive M4 stars.

1.4. Interpretation of RAC Slopes for Stars with Low- and High-activity

If there exists an interface between radiative core and convective envelope in any particular lower main sequence, magnetic activity may be powered by an $\alpha\Omega$-dynamo provided that rotational conditions at the interface are favorable (e.g., Mullan et al. 2015). If such a dynamo is in operation in a star, the magnetic activity would be expected to show some indications of being sensitive to rotation, i.e., at least some physical quantity that is associated with the "strength" of the dynamo should increase relatively steeply as Ω increases. In an RAC plot, such behavior would manifest itself as a relatively steep slope. The physical quantity that we favor in the present paper to be representative of the dynamo "strength" in lower main-sequence stars is the flux F(Ca II) of chromospheric emission in the Ca II resonance lines. This leads to an expectation that the RAC for a sample of such stars should have a relatively steep slope. H17 suggested that this could explain the maximally steep RAC slopes, which they obtained in dK4e, dK6e, and dM2e stars. We note the significant point that stars with spectral types K4, K6, and M2 are believed (see, e.g., Mullan et al. 2015) to have masses that are indeed large enough that a radiative core persists in the central regions of the star (Stromgren 1952; Osterbrock 1953), i.e., an interface dynamo is possible in such stars.

On the other hand, an α^2 dynamo is expected to be at least in principle capable of operation in *all* low-mass stars because the convective envelope in such stars occupies at least 50% (and in some cases 100%) of the volume of the star. H17 suggested that in the inactive dK4-dM2 stars, the fact that we observe the RAC slopes to be maximally shallow, and significantly (at greater than the 3σ level) shallower than the RAC slopes for the dK6e-dM2e stars, may be attributed to the operation of an α^2 dynamo (with its reduced sensitivity to rotation: Durney et al. 1993) in dK4-dM2 stars.

However, in stars where TTCC has occurred, i.e., the convective "envelope" expands to occupy the entire star, the interface is nonexistent, and the $\alpha\Omega$-dynamo is not accessible at all. In such stars, an α^2 dynamo may provide the only option for dynamo activity. If this is the case, then the RAC slope for all stars should approach the shallow value that is characteristic of α^2-dynamo operation. This expectation is seen in Figure 1 above as regards M3 and M4 stars.

Based on this interpretation of the *slopes* of the RAC that are plotted in Figure 1, H17 concluded the following: the TTCC occurs at spectral subtypes between M2 and M3.

1.5. Can More Than One Dynamo Operate Simultaneously in a Given Star?

We have already mentioned that dynamos of various types may operate in stars: $\alpha\Omega$, α^2, and $\alpha^2\,\Omega$. Is it possible that more than one of these may be operative in a star at an given time? To address this, we note that axisymmetric mean-field dynamo

models are described by two coupled equations for the field B and for the vector potential A: e.g., see Equations (24) and (25) of Charbonneau (2014). Source terms in both of these equations are ultimately responsible for modeling the driving of the dynamo. In the equation for A, only one source term exists: it includes the kinetic helicity parameter α. Because only one source term exists for A, the parameter α plays a crucial role in dynamo action; hence, the appearance of at least one power of α in each of the three possible dynamo types. In the equation for B, two source terms S_1 and S_2 are available: S_1 requires the presence of rotational shear (grad Ω), while S_2 relies on the presence of a nonzero value of α. Depending on the parameters in any particular star, either S_1 or S_2 can be omitted (but not both), and dynamo action may still occur. If S_2 is omitted, but S_1 is retained, the dynamo is labeled an $\alpha\Omega$ dynamo. If S_1 is omitted, but S_2 is retained, the result is labeled an α^2 dynamo. If both S_1 and S_2 are included, the result is labeled an $\alpha^2\,\Omega$ dynamo.

In principle, given the structure of the dynamo equations, there seems to be no mathematical reason to state that it would be impossible for two or three of these dynamos to be operating simultaneously in any given star.

Is there any empirical evidence that more than one dynamo is actually at work in a star? As far as we know, no such possibility has yet been reliably reported for the stars of interest to us in the present paper, i.e., K and M dwarfs. However, in the case of the Sun, the possibility of a double dynamo has been raised. Benevolenskaya (1995, 1998) analyzed solar magnetograph data from two complete solar cycles and reported evidence for two main periodic components: one at low frequencies, with a 22 yr period, and a second at high frequencies, with a "quasi-biennial" period (i.e., about 2 yr). (Analysis of an extensive data set, spanning 160 yr, of geomagnetic effects associated with solar activity, indicates that the high-frequency component may range in period from 1.2 to 1.8 yr: Mursula et al. 2003.) Benevolenskaya (1998) suggested that, based on an idea of Parker (1979), two spatially separated dynamos may be operating in the Sun: the 22 yr component near the base of the convection zone (where the radial gradient of Ω is large), while the 2 yr component operates near the surface (where the latitudinal gradient of Ω is large). Theoretical support for this possibility has been reported by Mason et al. (2002) and by Brandenburg (2005).

In view of these results, we should not be surprised if, in any particular K or M dwarf, two different dynamos might be found to be operating simultaneously. If the work of Benevolenskaya (1998) is any indication, the best way to detect two dynamos in a star might be to discover two well-defined periods in the activity cycle of that star. How much difference might exist between such double periods? If the Sun is any indication, the periods might differ by a factor of order 10. Is such a factor detectable in stellar data? To address this, we note that the largest survey of activity cycle periods in low-mass stars that is currently available (for more than 3000 stars) relies on *Kepler* photometric data, which vary on rotational scales (days) as well as on activity cycle scales (years; Reinhold et al. 2017). In the *Kepler* sample, most of the stars are found to have activity cycles in the range 2–4 yr. If a second period is present at 0.1 times the activity cycle, this period could be as short as 70 days: identifying such a short period against the background of rotational modulation (with periods in the range 10–40 days: see Reinhold et al. 2017) could be challenging. Nevertheless, it will be interesting to see if, as more data accumulate on activity cycles, any evidence emerges for double periods in the photometric data.

1.6. GAIA *Gap*

Jao et al. (2018) have reported, in a sample of some 700,000 *GAIA* stars within 100 pc, that there exists a gap, i.e., "a small slice of the HR diagram", which is less populated than surrounding regions in the HRD. The slice lies at an absolute K magnitude of +6.7 with a width of only 0.05 mag. The slice overlaps in color with single stars having spectral types of M2.0V, M3.0V, and M4.0V. Jao et al. noted that the gap lies near the regime where M dwarfs "transition from partially to fully convective, i.e., near spectral type M3.0V." Although Jao et al. do not refer to H17, we consider it remarkable that the spectral range M2-M3, which H17 identified as the range where chromospheric heating undergoes a significant change in properties, overlaps with the range of spectral types associated with the *GAIA* gap. This overlap encourages us to undertake a more extensive study of the Ca II emission properties than was possible at the time the H17 paper was written: the goal, as in H17, is to determine if there exists an observational signature in Ca II data associated with what Jao et al. describe as the transition from partly to fully convective, and H17 refer to as the TTCC.

Further reasons to explore empirical data sets in the vicinity of the TTCC for tell-tale signatures of the TTCC are provided by theoretical modeling of M dwarfs. Using a fine grid of stellar models, Van Saders & Pinsonneault (2012: VP12) discovered that, "near" the TTCC, an instability driven by He^3 can occur if the (deep) outer convective envelope comes into contact with a (small) convective core. Results for models with masses of 0.35–0.38 $M_\odot$ indicated oscillatory behavior in radii and luminosity. However, the information provided in the VP12 paper does not allow us readily to make comparisons with luminosities or spectral types of the relevant stars.

On the other hand, MacDonald & Gizis (2018: MG18) have presented models that clearly demonstrate a dip in the luminosity function at $M_K = +6.7$, with a width of close to 0.05 mag, thereby replicating very well two of the empirical features of the gap discovered by Jao et al. (2018). MG18 find that the narrowness of the gap is associated with the narrow range of stellar masses (between 0.315 $M_\odot$ and 0.345 $M_\odot$) over which there can be a merger between convection zones in the core and in the envelope. Their (implicit) computing method prevents them from identifying any oscillatory behavior of the type reported by VP12. J. MacDonald (2019, personal communication) has informed us that, in the range of masses where the merger occurs, his models have $T_{\rm eff}$ ranging from 3450 K to 3480 K: referring to Luhman et al. (2003), MacDonald reports that this corresponds to a spectral type near M2.5.

This is a significant result in the context of H17 where we were interested in the possibility of dynamo activity in our sample stars especially in the spectral range M2 to M3. In H17, however, we simplistically assumed a specific possibility, i.e., we thought that an $\alpha\Omega$ dynamo could operate effectively in a star lying above the TTCC, but would cease operation in a star lying below the TTCC. Now, however, in light of the VP12 and MG18 modeling, we are faced with a more complicated transition. The existence of an $\alpha\Omega$ dynamo has traditionally been associated with the interface (tachocline) between the

bottom of the outer convection zone and the *top* of the inner radiative region (Spiegel & Zahn 1992). But the models of VP12 and MG18 indicate that we now need to confront the fact that there can be a *second* interface lying much deeper inside stars with low enough mass: this second interface occurs between the *top* of the (small) inner convective zone (core) and the *bottom* of the interior radiative region. According to MG18, for stars with masses between 0.31 and 0.34 $M_{\odot}$, such a second interface is predicted to exist for timescales ranging from less than 1 b.y. for the 0.31 $M_{\odot}$ star, to as much as 9 b.y. for the 0.34 $M_{\odot}$ star. Thus, the existence of such an inner interface is guaranteed for a significant fraction of the age of the universe for M dwarfs in the appropriate mass range. Could a second tachocline exist at the second (inner) interface? And if dynamo activity were to occur in such a tachocline, would the fields thereby generated ever be able to rise to the surface, eventually contributing to chromospheric heating? We have already argued (Mullan et al. 2015) that magnetic fields generated at a deep tachocline in a K or M dwarf can indeed by buoyed up to the surface even if the tachocline is located quite close to the center of the star. Therefore, it is at least possible that the existence of a second tachocline in M dwarfs could contribute to magnetic fields at the surface of the star: the presence of such fields, lasting for a time of billions of years, could complicate the response of the chromosphere to magnetic heating. Instead of a sharp transition at a single spectral type, we may need to confront the possibility that the transition might be somewhat smeared out, depending on the age composition of the sample of stars we are examining. In particular, since more massive stars (i.e., 0.34 $M_{\odot}$) do not become fully convective for about 9 b.y., whereas the less massive stars (0.31 $M_{\odot}$) lose their "inner tachocline" in the course of a much shorter time (about 1 b.y.), we expect that the *more massive* stars will retain their extra interface "inner" dynamo for a longer time. This would skew the effects of chromospheric heating to last longer in somewhat more massive stars, i.e., those with *earlier* spectral types. To the extent that this is valid, our attempt to identify a signature of TTCC using chromospheric data could be shifted to somewhat earlier types than the spectral type at which the transition to full convection based on a global parameter such as luminosity occurs. Thus, while Jao et al. (2018) indicated that the *GAIA* gap (based on luminosity) is centered in stars with spectral type M3.0, our use of a chromospheric signature (based on magnetic effects at the inner tachocline) might be centered at an earlier type, i.e., closer to M2.0.

But in any case, if the *GAIA* gap is indeed associated with the presence of double convective regions inside an M dwarf (as interpreted by MG18), then the transition in chromospheric heating between the presence/absence of an $\alpha\Omega$ dynamo should occur at a spectral type that is close to that defined by Jao et al, i.e., in the range M2.0-M4.0.

1.7. Absolute Level of Ca II Emission as a Function of Spectral Type: Old Data

In the present paper, we are especially interested in the amount of mechanical energy that heats the chromosphere in our target stars. As well as being interested in the slope of the RAC, we are also interested in the magnitude of the Ca II emission flux that is present in each of our spectral sub-samples of K and M dwarfs. In Figure 2 (extracted from a figure in H17), we present an overview of the behavior of the absolute fluxes of Ca II emission in stars of increasingly late spectral

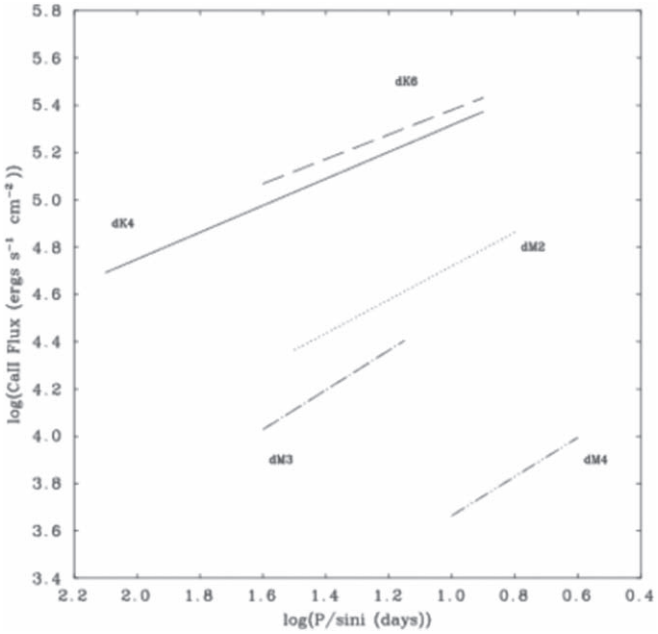

Figure 2. From H17: the flux of Ca II emission as a function of rotational period for a sample that contains only low-activity stars (dK, dM).

type. However, since we are interested here in comparing the data with theoretical models of acoustic flux, we restrict the data in Figure 2 to include only the *low*-activity stars (with spectral types dK and dM). As H17 have pointed out, the data for these stars indicate that there is a systematic decline in Ca II emission flux as we proceed from mid-dK to dM4. For our low-activity stars, the results in Figure 2 demonstrate that the decline in going from mid-K to M4 at a given rotational period amounts to a factor of 10 or more. Over the narrower range between M2 and M3, the Ca II emission flux declines (at a given period) by a factor of about 2.

In terms of the absolute level of Ca II emission in the stars in the H17 sample, we can use the results in Figure 2 to prepare for a subsequent (see Section 3 below) comparison with theoretical estimates of acoustic fluxes. In this regard, we note that the slowest rotators among the (inactive) dM2 and dM3 stars in Figure 2 have empirical fluxes F(Ca II) (in units of erg cm^{-2} s^{-1}), which are in the range from log F(Ca II) $\approx$ 4.0 to log F(Ca II) $\approx$ 4.3. By definition, the stars in Figure 2 (all of which are assigned to the category of *low*-activity stars) exhibit no detectable chromospheric *emission* in the Hα line. As a result, the most prominent emission features in the visible spectra of the dM2 and dM3 stars in Figure 2 are the Ca II H and K lines. In light of this, it might seem at first glance that the values of log F(Ca II) = 4.0–4.3 could be regarded as a zeroth-order estimate of the mechanical energy fluxes, which are heating the chromospheres in the inactive M2 and M3 stars.

Unfortunately, this conclusion is subject to serious limitations: the absence of Hα *in emission* in M dwarfs is *not* an unambiguous indication that chromospheric heating is absent. Because Hα is not a resonance line but requires population to be built up in an excited state, it is known theoretically (Cram & Mullan 1979; Cram & Giampapa 1987; Houdebine & Stempels 1997) and observationally (Stauffer & Hartmann 1986; Houdebine & Stempels 1997) that, in the atmosphere of an M dwarf, when the flux of mechanical energy is not too large, the resulting chromospheric heating can enhance the *absorption profile* of Hα without driving the line profile into

emission. Without access to detailed modeling, there is no simple method to quantify the mechanical energy fluxes that are needed to explain the empirical amounts of Hα *absorption* in any given inactive M dwarf. To be sure, in an active dMe star, the mechanical fluxes are certainly larger than in an inactive dM star. One example of the requisite quantitative modeling in two dM1 stars, one active, the other less active, has shown (Houdebine 2010) that the energy required to explain the Hα profile exceeds the energy required to account for the Ca II H and K lines (plus the Ca II infra-red triplet) by a factor of several.

Furthermore, there are other spectral lines in inactive stars where chromospheric emission is present, e.g., Lyα and Mg II. Regarding Lyα, Doyle et al. (1994) have argued that if a basal flux exists in this line in inactive M dwarfs, it is no larger than log F(Lyα) = 2.9: we can safely neglect this value compared to those of log F(Ca II). As regards Mg II emission, Mathioudakis & Doyle (1992) have reported that the basal fluxes in Mg II in M dwarfs with spectral types of interest to us here lie in the range log F(Mg II) = 4.0–4.3: this is essentially identical to the F(Ca II) fluxes in the most inactive stars in Figure 2. To account for radiative losses from other lines of Mg II and Ca II, Rammacher & Ulmschneider (2003) used fully time-dependent NLTE calculations of the solar chromosphere to show that all line emissions from Mg II exceed those in the Mg II k line by a factor of 1.4, and all line emission from Ca II exceed those in the Ca II K line by a factor of 4.3. Houdebine (2010) applied semi-empirical modeling to a dM1e star and found that when all emission lines are combined, the total requisite mechanical energy flux exceeds the Ca II fluxes by factors of 10 or more.

Moreover, it is not merely the obviously chromospheric emission lines that must be assessed for mechanical energy deposition: many photospheric absorption lines in the spectrum of an active M dwarf can be partially filled in as a result of chromospheric heating (Houdebine 2010). When model atmospheres are used to quantify the mechanical energy required to fill in the many photospheric absorption lines, Houdebine (2010) found that the total mechanical energy flux exceeds that observed in the Ca II H and K lines (plus the energy required for the infra-red Ca II triplet) by factors of x = 10–100. Reliable values of x are available only for two more or less active dM1 stars. In the case of inactive M dwarfs, quantitative information is not yet available about the filling-in of photospheric lines by chromospheric heating; however, in such stars, the value of x is almost certainly smaller than the above factors. Thus, in the inactive M dwarfs, the x factor may be less than 10.

As a result, although it would certainly be advantageous to have access to a simple formula that states, e.g., that the total mechanical energy flux F(mech) = x times the flux in Ca II H and K emission, such a formula is difficult to rely on in practice: the factor x can apparently be as large as 10–100 in the most active M dwarfs (Houdebine 2010), or probably less than 10 in the inactive M dwarfs. In view of this, we consider it very difficult to convert our measured Ca II H and K fluxes to an *absolute value of* F(mech) in any particular star. If such absolute fluxes *could* be obtained, it would be interesting to compare them with theoretical fluxes of acoustic waves. In Section 3 below, we describe the theoretically predicted acoustic fluxes as a function of $T_{\rm eff}$. However, our inability to make comparisons of *absolute values of F(mech)* need not preclude us from undertaking a *differential study* of the following kind: how much do the Ca II H and K fluxes *vary* as we move from one spectral type of M dwarf to a closely neighboring spectral type? After all, the observational signatures of mechanical energy deposition in emission and absorption lines in any particular star scale essentially with the *temperature gradient* in the chromospheric structure of that star (Houdebine 2010). In view of this underlying scaling, if we can identify *changes in* the Ca II line fluxes from one spectral type to another, these changes should provide (at least roughly) some estimates of the *changes in the* total F(mech) between one spectral type and another. In a *differential study*, there is no need to make individual measurements on *all* of the lines that are affected by the mechanical heating of the chromosphere.

But before undertaking such a differential study, we first turn to the new data that we have now obtained concerning F(Ca II) emission in a larger sample of M dwarfs: we examine the new data to see if they can strengthen the dynamo conclusions we have drawn from the RAC slopes.

2. Expansion of Our Sample to a Larger Number of Stars

In order to go beyond the results presented in H17, one of the authors (ERH) has recently expanded the sample of Ca II surface flux measurements to (roughly) 600 M1-M8 dwarfs, including (about) 130 dM2 stars. The latter number is a factor of two larger than the sample of M2 stars that was used in H17. In Figures 3–5, we present the Ca II fluxes (in units of erg cm^{-2} s^{-1} Å^{-1}) as a function of $T_{\rm eff}$ for the M stars in our expanded sample. We present the data in three separate plots in order to highlight certain properties of the data. In Figures 3 and 4, the plotted points refer only to *inactive* stars, i.e., those with spectral types dMx. In the figures, x is a number with two significant digits, i.e., we identify each star by its spectral sub-subtype. The difference between Figures 3 and 4 has to do with the bin sizes in spectral sub-subtype that are used for plotting. The bins in Figure 3, between M1.0 and M4.3, are chosen to include stars with only a single sub-subtype: at later spectral types, in order to have enough stars in the sample, the bins in Figure 3 are widened to include more than one sub-subtype. In Figure 4, all of the bins are wider than in Figure 3: between M1.0 and M4.5, bins in Figure 4 are chosen to include stars spanning a range of four sub-subtypes: at later spectral types, the bin sizes are expanded to include more than four sub-subtypes. In Figure 5, the plotted points refer to *active* M stars, i.e., those with spectral types dMex: in this figure, between M1.0 and M 6.0, we use the same (larger) bins as those in Figure 4. Note that the vertical scale on Figure 5 is 10 times larger than the scales in Figures 3 and 4: this indicates that active dMe stars emit almost an order of magnitude more flux in Ca II H and K than the inactive dM stars do.

A note on error bars. In Figure 3, each error bar has a length equal to a certain standard deviation σ. It is important to note that this σ is *not* a measure of the error in the empirical measurement of an individual Ca II line flux: such fluxes are actually quite well defined, and the measurements can be made with errors of typically no more than 10%–20%. Instead, the σ in Figure 3 arises from the fact that our Ca II fluxes represent averages over multiple flux measurements (typically dozens: see Section 1 above). Each dot plotted in Figure 3 indicates the mean Ca II flux of all available observations of dM stars with a particular spectral sub-subtype, while the error bars associated with each dot indicate the standard deviation of the scatter of all

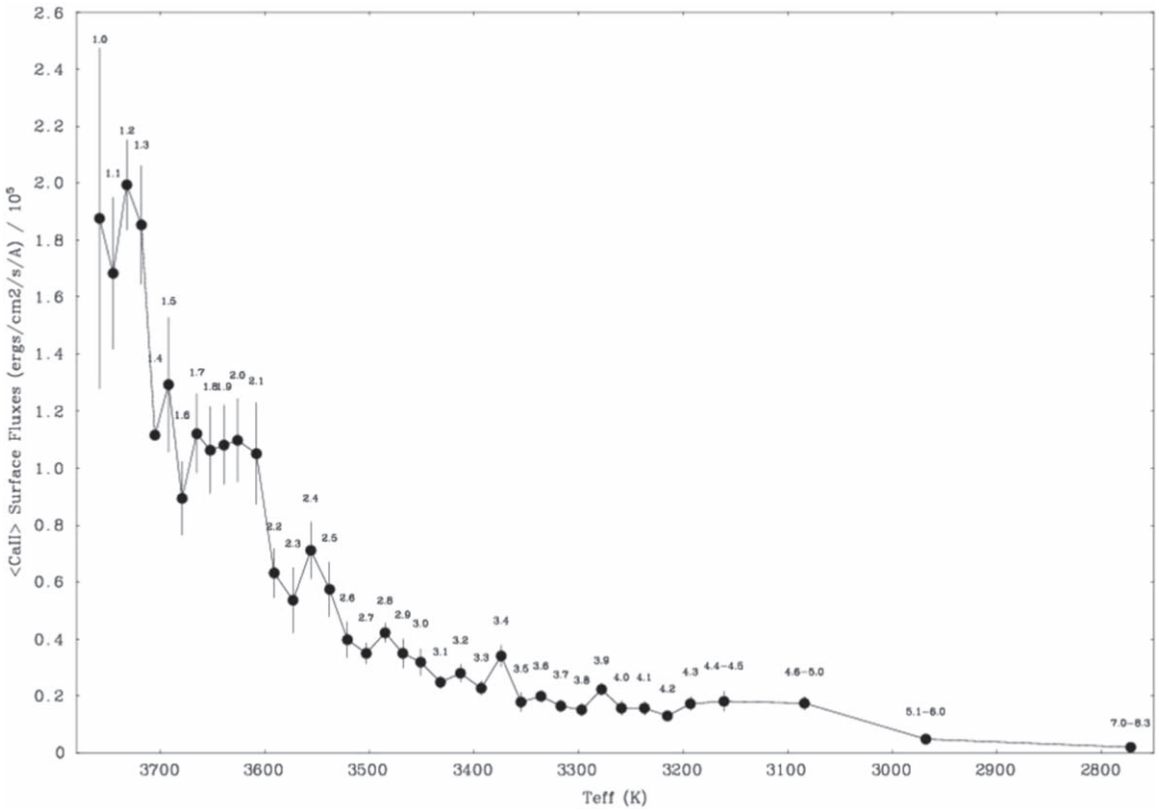

Figure 3. New data: measurements of Ca II surface fluxes vs. effective temperature for (inactive) M1-M8 stars. The data are plotted in narrow bins of spectral type, in steps of 0.1 times the subtype. Each plotted point is labeled with the spectral sub-subtype of the stars that contribute to that data point.

measurements at that sub-subtype about the mean. In Figures 4 and 5, the error bars represent 3σ, where the value of σ is once again a measure of the scatter of multiple measurements about the mean.

In plotting the data, we have used, as abscissa in Figure 3, the values of effective temperatures of stars that were at first estimated from $(R-I)_C$ colors. The measurements of stellar colors are now accurate enough that the numerical values of $(R-I)_c$ are reliable to three significant digits. Using these colors, Houdebine et al. (2019) have reported on a transformation from $(R-I)_C$ to T(eff), which, when averaged over our sample of hundreds of M dwarfs, leads to a formal 3σ error of ± 39.4 K in T(eff) for M dwarfs. In the present paper, where we quote values of $T_{\rm eff}$ to only three significant digits, we round up the formal estimate to $3\sigma = \pm 40$ K.

It is important to note that in deriving values of $T_{\rm eff}$ for each of the stars in our sample, the $(R-I)_c$ colors were used only as a first step. Our final estimates of $T_{\rm eff}$ (Houdebine et al. 2019) were obtained by taking the means of the $T_{\rm eff}$ values that we derived from $(R-I)_c$ plus mean values of $T_{\rm eff}$ that have been independently reported in the literature. The quoted uncertainty ($3\sigma = \pm 40$ K) is the mean of the difference between these two independently determined temperatures. However, recognizing the difficulties associated with the transformation from color to temperature, and with a view to being appropriately conservative, we can speculate about the possibility of a twofold larger value for the uncertainty: $3\sigma \approx 80$ K. This would yield $\sigma \approx 27$ K. We may ask: is a photometry-based value of $\sigma \approx 27$ K in $T_{\rm eff}$ plausible for M dwarfs? To answer this, we note that Kuznetsov et al. (2019) have recently reported on a sample of 420 M stars, for some of which they list values of $T_{\rm eff}$ based on photometry. For *individual* stars, they list σ values that range from about 40 to 150 K. The average value of σ for an individual M star in the Kuznetsov et al. sample is of the order of $\sigma(1) \approx 90$ K. In our analysis, rather than dealing with individual stars, we work with multiple stars in our sample at every sub-subtype: the number of stars that we have in each spectral sub-subtype can be estimated roughly from Figure 4, where we give the number of stars in each of our groupings of four sub-subtypes. Between M1.8 and M3.3, the average number of our sample stars in each sub-subtype is of the order of $n = 10$. The mean $\sigma(n)$ value for each sub-subtype is therefore $\sigma(n) = \sigma(1)/\sqrt{n} \approx 30$ K. Thus, even allowing for a twofold larger value for our uncertainties than the formal value, our estimated uncertainty of 27 K for our samples of multiple stars in each sub-subtype is roughly consistent with the photometry-based results reported by Kuznetsov et al. (2019).

We note that an uncertainty of 27 K in $T_{\rm eff}$ is typically the temperature difference between two adjoining spectral sub-subtypes (i.e., between, say, a star of type M2.2 and a star of type M2.3). When we rely on $(R-I)$ colors in the literature, some of these values are reported in the $(R-I)_K$ system: the formulae that transform the $(R-I)$ colors from the Kron system to the Cousins system yield uncertainties of $\approx$0.002 mag (Leggett 1992). So when we start with $(R-I)_K$ measurements and transform to $(R-I)_c$, no significant error is incurred. A source of more significant uncertainty is the presence of temporal variations of the $R-I$ color due to activity. However, multiple measurements of $R-I$ are available for many of our stars, and averaging allows us to reduce the activity-related variations. In particular, in low-activity stars (i.e., most of the stars in our sample), the

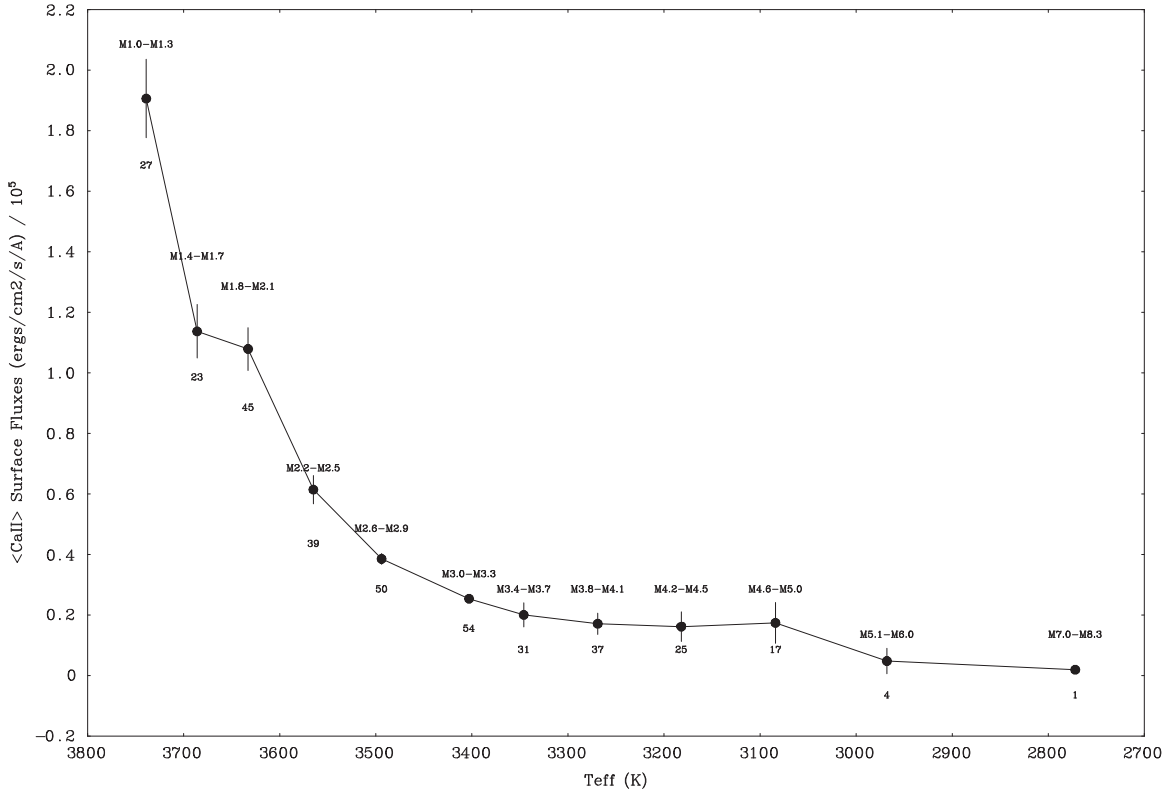

Figure 4. New data: measurements of Ca II surface fluxes vs. effective temperature for (inactive) M1-M8 stars. The data are plotted in larger bins of spectral type, spanning four sub-subtypes. Each plotted point is labeled with the range of spectral sub-subtype of the stars that contribute to that data point. For each point, the number that appears underneath the lower error bar of each point indicates the number of stars in our sample that were used to calculate the data for that point. The largest sample occurs in the bin M3.0-M3.3. The scale along the vertical axis in this figure is the same as that in Figure 3.

variations in $(R - I)$ reported by different observers at different times are typically of the order of 0.01 mag. Therefore, when we compute averages of the color, temporal variability in $R - I$ (although real) is not a significant source of uncertainty in the low-activity stars that dominate our sample. The principal source of uncertainty in our analysis arises from the calibration of the relationship between $R - I$ and $T_{\rm eff}$: in this relationship, a large contribution to scatter is due to variations in the metal abundances [M/H] from star to star. In order to minimize these effects, we have excluded subdwarfs from our sample.

For the stars of greatest interest to us here, i.e., those with spectral types M1-M3, the $(R - I)_{\rm C}$ colors reported by Houdebine et al. (2019; see their Figure 3) span a range from roughly 1.0 to 1.5. The corresponding range of T(eff) values is roughly 3750–3400 K, i.e., a range of 350 K. If we wished to define T(eff) values with a formal statistical significance of 3σ (=40 K), we could accommodate about nine subdivisions of spectral types into the range of 350 K. In grouping the stars in Figure 3, we have in fact selected 20 spectral subdivisions between M2.0 and M3.9, i.e., we have divided the stars into bins each of which spans one-tenth of a spectral subtype (for convenience, we define this as one spectral sub-subtype). For the center of each bin, we have selected the $T_{\rm eff}$ value for each sub-subtype. Thus, the statistical significance of the $T_{\rm eff}$ values in each of our sub-subtypes is not as large as the formal 3σ error mentioned above: instead, each bin corresponds to one-half of the formal error, i.e., about 1.5σ. Although we do not label any of the dots in Figure 3 to indicate our sample size within a single bin, the sample sizes within the four-fold wider spectral bins as plotted in Figure 4 are as follows: M1.0-M1.3 (sample size = 27), M1.4-M1.7 (23), M1.8-M2.1 (45), M2.2-M2.5 (39), M2.6-M2.9 (50), and M3.0-M3.3 (54).

A feature in Figure 3 to which we will draw attention in what follows (see Section 2.2) is the relatively sharp decrease in flux between M2.1 and M2.2. The presence of such a sharp decrease suggests that we can be rather confident in the $T_{\rm eff}$ values derived by Houdebine et al. (2019) where the estimated uncertainty in $T_{\rm eff}$ indicated that we could assign spectral types with a confidence of 1–2 sub-subtypes. If our assignments had been subject to uncertainties that are larger than 1–2 sub-subtypes, then the sharp decrease in Figure 3 between M2.1 and M2.2 would have been "smoothed out" due to the incorrect random assignment of stars over several sub-subtype bins. An anonymous referee has questioned the argument in the present paragraph in the sense that it may involve "a form of circular reasoning and/or confirmation bias"; however, in Section 2.2 below, we shall present in Figure 4 the same data that appear in Figure 3 except that in Figure 4, the data will be plotted in wider bins. It is important to note that some of the features that we highlighted in Figure 3 carry over into Figure 4: the referee considers that such a result "provides a more convincing argument" for the validity of our assignment of sub-subtypes.

In a similar vein, the bins in Figure 3 were selected such that the center of each bin is placed at a single value of the spectral sub-subtype. How sensitive might the shape of the plot in Figure 3 be if we were to shift the bin centers? If all errors in our assignment of spectral type are random, then shifts at the level of one sub-subtype out of a bin in one direction could be compensated by more or less equal shifts in the opposite direction. In such a case, the features ("dips") in Figure 3 would persist. However, if systematic effects are present

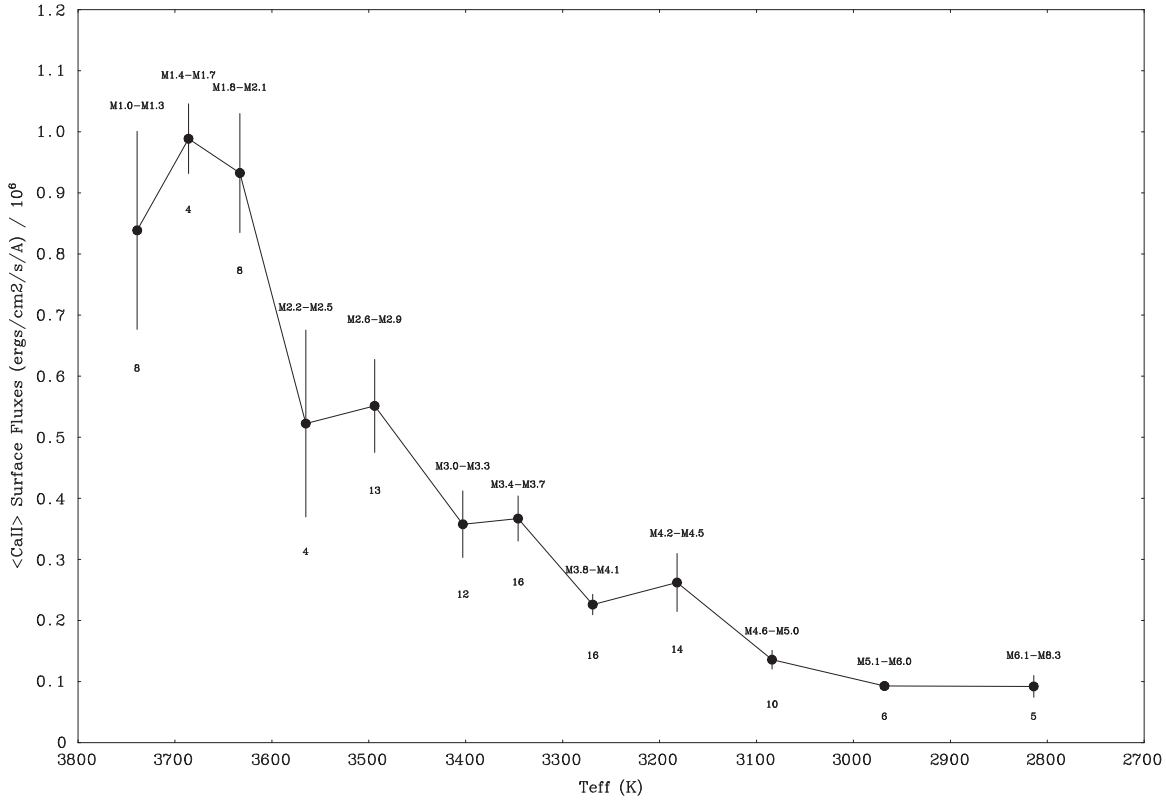

Figure 5. New data: measurements of Ca II surface fluxes vs. effective temperature for (active) M1e-M8e stars. The data are plotted in the same (larger) bins of spectral type as in Figure 4. The flux units on the vertical axis are 10 times *larger* than those in Figures 3 and 4.

(although we are not aware of any such), the compensation might not be exact, and this could introduce spurious "dips" and "pile-ups" in the plots. To address this possibility, we show in Figure 4 what happens to the data in Figure 3 when the bins are widened by a factor of four. It seems quite unlikely that any errors in spectral type assignment could be as large as four sub-subtypes. Therefore, the plot in Figure 4 is much less likely to suffer from errors due to a star mistakenly being plotted in the "wrong" bin. In this regard, it is important to note that we shall find (in Section 2.2 below) that at least one of the dips in Figure 3 (namely, the one between M2.1 and M2.3) persists in Figure 4. This helps to improve our confidence in the reality of that particular dip.

We now wish to draw attention to certain aspects of the data in Figure 3.

2.1. Overall Decline in Ca Emission Flux toward Later Spectral Types

It is obvious that there is an overall decline in F(Ca II) as we consider stars of increasingly late spectral types. That is, the flux of mechanical energy that is heating the chromosphere decreases as the spectral type increases. Now, the flux of mechanical energy that is available for chromospheric heating is derived ultimately from the bolometric luminosity, which emerges from the star in radiative form. The ratio of F(Ca II) in any particular star to the bolometric flux $F\,(\mathrm{bol}) = L_{\mathrm{bol}}/4\pi R_*{}^2$ of that star is a measure of the fraction f_{mech} of the stellar output, which is converted into mechanical form, to be deposited eventually into the chromosphere. The data in Figure 3 enable us to address the following questions: Does f_{mech} vary with spectral type? Or does f_{mech} remain constant in stars with different spectral types?

To address this, we note that F(bol) can be written as $\sigma_{\mathrm{B}} T_{\mathrm{eff}}{}^4$ where σ_{B} is the Stefan–Boltzmann constant. In order to determine how f_{mech} varies with spectral type, let us consider two sample spectral types: M1.5 and M4.2. For these two types, T_{eff} has values of roughly 3750 and 3250 K (Houdebine et al. 2019). Thus, F(bol) has numerical values of 1.1×10^{10} and 6.3×10^{9} erg cm^{-2} s^{-1} at spectral types M1.5 and M4.2.

Regarding the fluxes F(Ca II), the data in Figure 3 (and assuming a line width of 1 Å) indicate that at M1.5, the mean $F(\mathrm{Ca\ II}) = 1.3 \times 10^{5}$ erg cm^{-2} s^{-1}, while at M4.2, $F(\mathrm{Ca\ II}) = 0.12 \times 10^{5}$ in the same units. Thus, at M1.5, $f_{\mathrm{mech}} = 1.2 \times 10^{-5}$, while at M4.2, $f_{\mathrm{mech}} = 1.9 \times 10^{-6}$. These numbers show that the efficiency of chromospheric heating decreases by a factor of about six as we go from M1.5 to M4.2. Our data indicate that the flux of chromospheric emission is *not* simply proportional to the bolometric flux: there is more going on in the process of chromospheric heating than simply siphoning off a fixed fraction of the available energy flux emerging through the surface of the star. Instead, the fraction of stellar energy flux that goes into chromospheric heating *decreases* at later spectral types. Later-type stars are apparently less efficient at generating mechanical energy from a given flux of radiant energy. If the total radiative losses $F(r)$ from the chromosphere are of order 10–100 times larger than F(Ca II), then $F(r)$ may have values in the range $1.3 \times 10^{6-7}$ at spectral type M1.5, and $F(r)$ may have values in the range $1.2 \times 10^{5-6}$ at spectral type M4.2. In these cases, f_{mech} may be as large as $1.2 \times 10^{-(3-4)}$ and $1.9 \times 10^{-(4-5)}$ at M1.5 and M4.2, respectively.

For comparison, in the quiet Sun (i.e., where heating is probably not dominated by magnetic effects), the total radiative

losses from the chromosphere amount to 4×10^6 erg cm^{-2} s^{-1} (Withbroe & Noyes 1977). Comparing this to $F(\mathrm{bol}) = 6.3 \times 10^{10}$ erg cm^{-2} s^{-1} for the Sun, we find $f_{\mathrm{mech}} = 6 \times 10^{-5}$ in the quiet Sun. Thus, red dwarfs with spectral types M1.5 and M4.2 are more efficient at heating the chromosphere than the quiet Sun by factors that may be as large as about 20 and 3, respectively.

2.2. "Dips" in the Decline in Ca Emission Flux toward Later Spectral Types

In Figure 3, we plot data for the (inactive) dM stars, using steps of 0.1 in spectral subtype. Examination of the plot suggests that, superposed on the overall decline in Ca II line flux toward later spectral types (described in Section 2.1), there may be some "fine structure." We wish to determine if this "fine structure" contains physically meaningful information, perhaps associated with the "switching off" of a dynamo mechanism.

At first glance, we note that, in the section of the curve between M1 and M3, "fine structure" might be present in the form of "dips" in the curve at M1.1, M1.4, and M1.6. However, some of these dips consist of only one data point: as a result, it is difficult to rule out the possibility that these are merely noise in the data. On the other hand, there are also dips in the curve that contain *two* consecutive low points, such as at M2.2, M2.3, and at M2.6, M2.7. It seems less likely that these can be considered merely noise.

In order to identify dips that may be distinguished from mere noise, we consider an argument that is suggested by an analysis that has been used to enhance the confidence of identifying *bona fide* flares in noisy photometric data (see Paudel et al. 2018). In the work described by Paudel et al., temporary increases in light level are observed from time to time against a background, which is essentially noise. Any particular temporary increase in light level *might* be due merely to noise, or it *could* be due to a *bona fide* flare. However, if two increases in the light level occur right next to each other, i.e., during two contiguous intervals of observing, the chances of those two increases in photometric level being a *bona fide* flare are significantly improved compared to the case of an isolated (single) increase in the photometric level. Paudel et al. use data on the amplitudes A_i, A_{i+1} of pairs of successive events and normalize each amplitude to the local standard deviation of the noise levels σ_i and σ_{i+1}. The product (A_i/σ_i) times (A_{i+1}/σ_{i+1}) is considered to provide a quantitative measure of the statistical significance of the possibility that a flare has in fact been detected. Let us consider two possible cases. In case (i), where all that is observed is a single "blip," the amplitude of that blip A_i may be large compared to σ_i, but the succeeding data point will have an amplitude A_{i+1}, which is small compared to σ_{i+1}. As a result, the product (A_i/σ_i) times (A_{i+1}/σ_{i+1}) in case (i) will turn out to be relatively small. In such a case, one concludes that a *bona fide* flare did not occur. On the other hand, in case (ii), where two successive amplitudes are observed to be large, then the product (A_i/σ_i) times (A_{i+1}/σ_{i+1}) is a relatively larger number than in case (i): in such a case, the chances that a flare really did occur are greatly improved. We do not claim that our approach here is as statistically rigorous as that described by Paudel et al. (2018): unlike Paudel et al., we do not have the luxury of dealing with a background that is essentially noise. Moreover, we are not dealing with a *time* series of data: instead, we are examining a series of data arranged in order to spectral subtype. Nevertheless, we consider that our examination of observations grouped in pairs of immediately adjacent spectral subtypes captures the spirit of the approach of Paudel et al. (2018).

With this in mind, we start with the data points in Figure 3, i.e., at each spectral sub-subtype, we have a value of the flux F_i and a value of its associated standard deviation σ_i. Using these, we calculate the difference between successive pairs of points $\Delta = F_i - F_{i+1}$ and then taken the ratio of Δ to the combined standard deviation $\sigma = \sqrt{(\sigma_i^2 + \sigma_{i+1}{}^2)}$. Examining the values of Δ/σ as a function of spectral type for evidence of "dips," we have no interest in pairs of data points for which Δ/σ is a *positive* number. Instead, we are most interested in those pairs of data points with the largest (in absolute terms) *negative* numerical value of Δ/σ. We find that the largest negative Δ/σ has a value of -2.9 for pair (a) at spectral sub-subtypes M1.3 and M1.4. The second largest negative Δ/σ has a value of -2.3 for pair (b) at spectral sub-subtypes M2.1 and M2.2. No other pair of successive points has a Δ value as large as 2σ. However, we note that pair (c) at M2.4-M2.5 and pair (d) at M2.5-M2.6 have Δ/σ values of -1.0 and -1.2, respectively. Now, we proceed to the second step of our calculation. We consider the product of the above largest values of Δ/σ with the value of Δ/σ for a neighboring pair. Combining pair (a) with the pair M1.2-M1.3, we obtain a product of the two neighboring Δ/σ values equal to $+1.8$. Combining pair (b) with the pair M2.2-M2.3, the product is found to be $+1.3$. And combining pair (c) with pair (d), the product is found to be $+1.2$. These are the only pairs for which the products are in excess of $+1$.

On the basis of this discussion, we consider that the best candidates for "dips" of interest in Figure 3 are as follows. The dips, which we label as Da, Db, and Dc, are found to occur at spectral types M1.2-M1.4, M2.1-M2.3, and M2.4-M2.6.

Now let us consider the data in Figure 4, where the same sample of (inactive) dM stars that were used for Figure 3 are grouped into wider bins. The use of wider bins has the effect that the standard deviation of each bin is smaller than those in Figure 3: the smaller values of σ will lead to (numerically) larger values of Δ/σ. For ease of reference, we will label the points in Figure 4 in order from left to right as A,B,C... Repeating the exercise described above, we find that the largest negative value of $\Delta/\sigma = -5.2$ occurs between points C and D. The next largest negative value of $\Delta/\sigma = -5.0$ occurs between points A and B. The remaining values of Δ/σ become progressively smaller (in magnitude) as we go beyond point D. When we take the next step in our analysis and calculate the product of Δ/σ for neighboring pairs, we find that the largest product of Δ/σ for neighboring pairs is $+21$ for the pair C-D and D-E. For the pair A-B and B-C, we find that the product is $+3$. These results suggest that the best candidate for a "dip" in Figure 4 extends from C (=M1.8–M2.1) to E (=M2.6–M2.9), with the largest "dip" occurring between C and D, i.e., between M1.8-M2.1 and M2.2-M2.5. Compared to the results in Figure 3, this range of "interesting" spectral types we have obtained from Figure 4 overlaps best with "dip" Db identified in Figure 3, although there is also some overlap with "dip" Dc. Our analysis of Figure 4 suggests that there is no significant overlap with "dip" Da in Figure 3.

Turning now to Figure 5, we examine the data for the (active) dMe stars, which are grouped into the same set of bins as were used in Figure 4. We will use the same notation as in Figure 4, labeling each point from left to right in Figure 4 as A, B, C... We recognize that our sample of dMe stars is smaller than for the dM stars, but we can repeat the analysis that we have applied to Figures 3 and 4. When we do that, we find that the largest (negative) numerical value for Δ/σ in the spectral range M1-M3 is found to be -2.3, between points C and D. We note that the largest value of Δ/σ that we found in Figure 3 also occurred between points C and D, just as we find in Figure 5. Moving on to the next step in the analysis, we find that the product of Δ/σ values for neighboring pairs, we find that the only case where the product is positive occurs for the pair C-D and B-C. Thus, the best candidate for a "dip": in Figure 5 extends from B (=M1.4–M1.7) to D (M2.2-M2.5). Compared to the results in Figure 3, we see maximum overlap with dip Db; there is less overlap with dip Dc but none with dip Da.

The data with the finest resolution (Figure 3) suggests that the best candidate for a significant "dip" lies between M2.1 and M2.3. This dip is consistent also with our analysis of Figures 4 and 5. For that reason, we consider that the range M2.1-M2.3 is the best candidate for the location of a change in dynamo mode among early M dwarfs. Whereas H17 suggested that the change in dynamo mode occurred between M2 and M3, we now suggest that we can narrow the range down to M2.1-M2.3.

3. Comparison with Theoretical Work: Basal Fluxes

In solar-like stars, and in lower-mass stars, it is well known, based on RAC data, that magnetic activity contributes to enhancements in chromospheric emission in the most active stars. However, an important empirical feature of the chromospheric data is that there exists a *lower limit* on chromospheric activity (as indicated by Ca II emission) in cool stars (Schrijver 1987; Rutten et al. 1991). As far as we know, there are no lower main-sequence stars with spectral types of K or M that exhibit *zero* chromospheric emission. The existence of a firm lower limit on chromospheric emission in cool stars led Schrijver and colleagues to the proposal that there exists a "basal flux" of energy that provides a "floor" on the chromospheric heating in all cool stars, even in the least active stars. Now a salient aspect of the sample of stars that have been analyzed in the present work is that, because they are extracted mainly from HARPS data (but also include data from FEROS, SOPHIE, NARVAL, and UVES), the sample of stars is somewhat biased toward low-activity stars. In light of this, we expect that some of the stars in our sample might have chromospheres that lie near the basal level.

In the context of low-activity stars, and because we are interested in pushing observations to the lowest possible limits of flux in the Ca II emission line, it might be asked: have any of our target stars been found to have *no* chromospheric emission in Ca II at all? This question can be answered definitively: in all 600 (or so) M dwarfs for which we have examined archival spectra from HARPS, FEROS, SOPHIE, NARVAL, and UVES, a measurable emission flux has been found in the Ca II line. The fact that in all 600 stars, chromospheric emission is measurable in Ca II suggests that chromospheric heating relies on a physical process that is present in all of the stars in our sample.

One feature that occurs in all M dwarfs is a deep convective envelope where pressure fluctuations are inevitably associated with convective overturning: these fluctuations generate acoustic waves with a range of periods, and waves of short-enough periods (i.e., shorter than the acoustic cut-off period: see, e.g., Mullan 2009) can provide a finite amount of mechanical flux to the chromosphere. This flux of short-period acoustic waves sets a firm lower limit on the mechanical energy flux, which is available to the chromosphere in any star with a convective envelope. The existence of a lower limit on the acoustic energy flux that reaches the chromosphere is consistent with the concept of a "basal flux" as proposed by Schrijver (1987). A natural question that arises is: Is there any justification for the possibility that "low activity" in an M dwarf can be considered as being equivalent to "near the basal level" of acoustic power? To test this, quantitative agreement between acoustic heating and the lowest empirical values of chromospheric emission have been reported by, e.g., Mullan & Cheng (1993) and Fawzy & Stepien (2018). To be quantitative, we note that the phrase "near the basal level" is defined as follows in the study by Mullan & Cheng (1993). An empirical value of the basal flux in Mg II emission had previously been reported by Rutten et al. (1991) as a function of $B - V$ color. For each target star in an available sample of 30 stars, Mullan & Cheng (1993) inserted the $B - V$ color in order to extract a Mg II basal flux. Then, the stars that were to be modeled with acoustic heating were selected to be no more than a certain limit above the basal flux. In order to obtain a sample of stars that was not too small, the limit was set at 0.9 in the log(flux). That is, the stars to be fitted were chosen to have Mg II fluxes, which exceeded the basal flux by less than one order of magnitude. Then, an acoustic model based on dissipation of weak shocks was fitted to the Mg II emission fluxes, as well as to the emission fluxes in Lyα. Satisfactory fits were obtained for both of these individual lines.

However, the work of Mullan & Cheng (1993) was published before it was realized that the total radiative losses from the chromosphere exceed those in individual lines by factors that range from a few up to values as large as 10 or more (Houdebine 2010). In light of the latter development, it no longer seems to be permissible to claim that acoustic power alone is sufficient to provide for the total radiation losses from the basal flux stars. It seems that something in addition to acoustic power may be required to explain the basal flux.

In order to address this with more precision, it is necessary to quantify in greater detail the acoustic energy fluxes that can be generated in the atmospheres of low-mass stars.

According to the work of Lighthill (1952) and Proudman (1952), the flux of acoustic power F_A, which is generated by turbulence in which the mean speed is v scales as v^8. Models of lower main-sequence stars (e.g., Castellani et al. 1971; Mullan 1971) suggest that the maximum convective velocity v(max) in the models of main-sequence stars has a well-defined behavior: there is a peak among A-type stars ($\log T \approx 3.9$), and then there is a monotonic decrease in v(max) as we go down the main sequence toward cooler values of T(eff).

Based on this, and adopting a model of turbulent eddy distributions in stars along the lower main sequence, a value can be calculated for the flux of acoustic power that is to be expected as we go to lower-mass stars on the main sequence. Extensive results have been presented by Ulmschneider et al. (1996) for a variety of surface gravities from $\log g = 0$ to $\log$

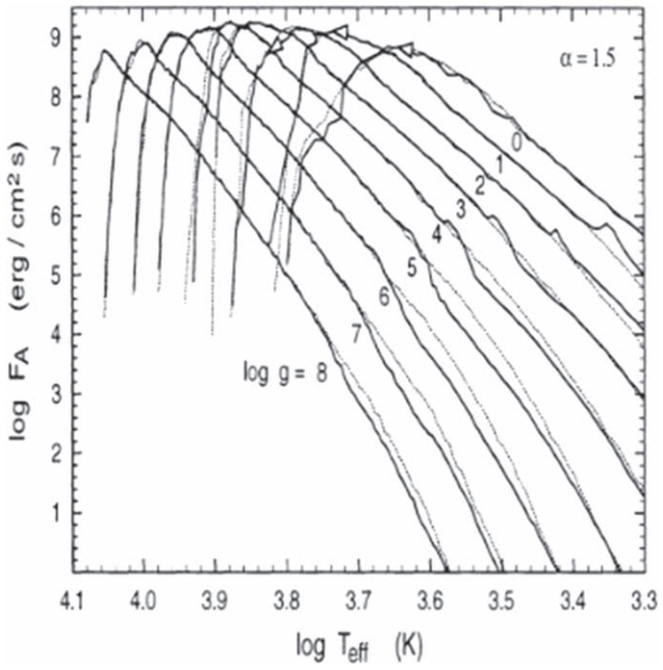

Figure 6. (From Ulmschneider et al. 1996) Theoretical evaluation of acoustic fluxes F_A emitted by stars with effective temperatures ranging from 2000 to 13,000 K and gravities in the range from log $g = 0$ to log $g = 8.0$. The solid lines represent acoustic fluxes from convective models computed with mixing length theory using a mixing length of 1.5 pressure scale heights. The dotted lines depict calculated fluxes neglecting the presence of H_2 molecules. We are especially interested in results with T(eff) values in the range log(T(eff)) = 3.53–3.57 and gravities of order log $g = 5$.

$g = 8$. A sample of their results is presented in Figure 6: the results in the figure refer to convective zone models, which are computed with a value of mixing length = 1.5 times the pressure scale height. In the present paper, we are interested mainly in stars with spectral types M0 to M7, where masses range from about 0.6M(Sun) down to about 0.1M(Sun). For such stars, the radius and mass are correlated according to $R \sim M^b$ where empirical data indicate that $b = 0.945 \pm 0.041$ (Demircan & Kahraman 1991). The surface gravity g therefore scales as $M^{-0.89}$. For the M stars, which are of the most interest to us, this leads to log g values in the range from 4.7 to 5.2.

The results in Figure 6 need to be handled with some caution. Although Ulmschneider was the lead author of the paper that generated the results in Figure 6, he and his colleagues, at a later date (2005), stated that the results "may" lead to an incorrect evaluation of chromospheric heating (Ulmschneider et al. 2005: U05). The results in Figure 6 were obtained by means of a 1D model in which multiple shocks merge into one another in the atmosphere of a star: such mergers are a natural occurrence if all gas motions are forced to be confined strictly to a single dimension. However, in the light of 3D considerations, U05 stated that shock merging is expected to occur only rarely. U05 emphasized that "adequate" calculations of chromospheric heating "require a 3D radiative-hydro code with multiple input sources of acoustic wave spectra," as well as a "fully time-dependent treatment of ... ionizations and thermodynamics." U05 stated that such calculations "are not yet feasible with present computer power." In a subsequent paper, Hammer & Ulmschneider (2007) indicate that 1D models (such as those in Figure 6) can describe strong brightenings in the chromosphere "quite well," but the "overall chromospheric dynamics" may be governed by 3D shock propagation.

Because of the complexities of the 3D problem (as stressed by U05), the results in Figure 6, spanning eight orders of magnitude in gravity and spanning almost the entire range of $T_{\rm eff}$ for main-sequence stars with convective envelopes, have never, as far as we are aware, been re-computed using a full 3D code. If such re-computations were to become available over the range of parameters shown in Figure 6, we would certainly like to compare the results with our observations of Ca II emission. In the absence of such results, the results in Figure 6 cover such a broad range of parameter space that they offer us an opportunity to be used in a narrowly confined *differential study of chromospheric heating,* at least for a zeroth-order approach to the problem. By "narrowly confined," we mean that our data are confined to a narrow range of log $T_{\rm eff}$ (3.5–3.6) and to essentially a single value of log g (5.0).

Using a mean value of log $g = 5$, we see in Figure 6 that the values of F_A have a peak at log $T \approx 3.9$, and F_A declines toward later spectral types. In the parameter range of interest to us here, i.e., log $T_{\rm eff} = 3.6$–3.5, and log $g = 5$, Figure 6 shows that F_A has values between (about) 10^5 and 10^3 erg cm^{-2} s^{-1}. We note that the values of F(Ca II) in our inactive sample stars (see Figures 3 and 4 above) range from about 2×10^5 and 1×10^4 erg cm^{-2} s^{-1}. Thus, the theoretical acoustic fluxes do overlap with the empirical Ca II emission fluxes. However, since the entirety of chromospheric heating requires an energy flux of x times F(Ca II), where x may range from as small as a few to as large as 10 or more, then the acoustic fluxes in Figure 6 *might not* suffice to account for the *mean level* of chromospheric heating. However, in this regard, it is worth noting that the data in Figure 4 represents *mean* fluxes for inactive dM stars: individual stars are scattered about the mean at each spectral type. In fact, M dwarfs with the lowest levels of activity, and also M subdwarfs (which were not used in forming the means in Figure 4), are observed to have Ca II fluxes that lie *below* the mean values plotted in Figure 4 by factors of 5–10 (E. R. Houdebine et al. 2020, in preparation). Such stars would be the best qualified to be labeled as basal flux stars, and they *could* be powered by acoustic fluxes.

If indeed acoustic power is not sufficient to power the mean levels of chromospheric heating in inactive M dwarfs, we need to ask: Where does the rest of the chromospheric heating come from in such stars? From observations of the Sun, it is well known that chromospheric heating is stronger in regions with stronger magnetic fields (Withbroe & Noyes 1977). In going from quiet Sun to an active region, the total radiative losses from the chromosphere increase by a factor of five. It seems likely that magnetic effects are also at work in heating the mean chromospheres in the inactive M dwarfs. Several magnetic processes have been proposed to heat stellar chromospheres, including transverse waves on a magnetic flux tube (Musielak & Ulmschneider 2002) and Alfvén waves (Cranmer & van Ballegooijen (2005). Other mechanisms include dissipation of electric currents (Goodman 1995) and nanoflares (Parker 1988; Jess et al. 2014). Unfortunately, making predictions based on magnetic effects requires the introduction of many more free parameters than the number that is required for the acoustic fluxes shown in Figure 6. As a result, the parameter space with two-dimensions ($T_{\rm eff}$ and g), which enabled Ulmschneider et al. (1996) to compute the results in Figure 6, must be expanded to a larger number of dimensions in order to include magnetic

effects. The expanded number of parameters includes at least the following: numerical values of the magnetic field strength, the topology of the field (open? closed? multipolar?), the fractional area of the surface occupied by fields, the efficiency of exciting each magnetic mode on a flux tube, the frequency spectrum of the waves that are excited (e.g., Cranmer and van Ballegooijen consider a spectrum extending from periods of 3 s to 3 days, i.e., a range of five orders of magnitude), the local geometry of the field lines that carry the wave upwards to the chromosphere (determining the effectiveness of refraction and reflection of the various modes of upward waves Osterbrock 1961), the process that allows each magnetic mode to dissipate in the chromosphere, the processes that enable dissipation of electric currents in a partially ionized magnetized plasma, and, finally, the dimensions in space and time and energy of nanoflares (Jess et al. 2014). This large array of unknowns pertaining to magnetic heating of the chromosphere gives rise to a parameter space that is so vast that exploration of even a small volume will require computing enormous effect. Many different combinations of these various parameters might eventually be found that agree with some of the data, but it is not clear how one will be able to decide which combination is the correct one for any given star. In contrast, the two-parameter space represented in Figure 6 contains information that can be meaningfully used to set at least a lower limit on the magnitude of the mechanical energy that is available for chromospheric heating.

4. Possible Origin of a "Dip" in Our Ca II Line Flux Data

With regards to the decline toward the later spectral type in Figure 6, it is worth noting the prominent "molecular feature" in Figure 6: two sets of results are presented, one plotted with solid lines, the other with dotted lines. The difference between these two sets has to do with the inclusion (solid lines) or non-inclusion (dotted lines) of H_2 molecules in the gas. In the case $\log g = 5$, which is the case of primary interest in the present paper, the molecular feature does indeed cause a significant decrease in the acoustic flux over a certain range of T(eff), namely, for $\log T$(eff) between (roughly) 3.65 and (roughly) 3.59. In this range of temperatures, the predicted value of F_A in the molecular inclusion model declines by a factor of about two relative to the non-inclusion model. At values of T(eff) lower than 3.59, i.e., after traversing the "molecular feature," the values of F_A for the inclusion model at $\log g = 5$ reverts to a steady decline as $\log T$(eff) decreases, with a slope that is essentially identical to the slope that was in place before traversing the "molecular feature."

With regards to the molecular feature, when we examine the stars that are of most interest to us in this paper, i.e., M1-M3 stars with T(eff) in the range of roughly 3750–3400 K (see Figure 3), we note that the corresponding values of $\log T$(eff) = 3.53–3.57 lie on the cool side of the "molecular feature" in Figure 6. As a result, we do not anticipate that the "molecular feature" should lead to any significant features in our data. On the contrary, we expect that the predicted values of acoustic flux F_A in our sample of stars should undergo a smooth steady decline as we go from the warm end of our sample ($\log T$(eff) = 3.57) to the cooler end ($\log T$(eff) = 3.53). In fact, over the range of T(eff) values that are of interest to us here, the predicted values of $\log F_A$ (with $\log g = 5$ in Figure 6) can be seen to decline smoothly from about 4.6 to about 3.8, i.e., by a factor of about five.

In this regard, we consider it a matter of some interest that, according to the results in Figure 6, as we go from a star with T(eff) = 3750 K to a star with T(eff) = 3400 K at $\log g = 5$, the theory suggests that the decline in F_A should be *smooth*, i.e., more or less monotonic. The predictions of F_A reported by Ulmschneider et al. (1996) do not indicate that there should be "dips" or "recoveries" in the decline. Admittedly, a careful examination of Figure 6 does show that, as we traverse the "molecular feature," there are two regions of the F_A curve for $\log g = 5$ (around $\log T$(eff) = 3.595 and 3.58) that have shapes that might be classified as plateaus.

In this regard, we wish to draw attention to the empirical features, or "dips", that we described in our data in Section 2.2 above. As mentioned there, we consider that the "dip" with the largest statistical significance is the one between M2.1 and M2.3. What could give rise to such a feature? We recall that the stars in our sample are low-activity stars: such stars are, in general, believed to be good candidates for acoustic heating of their chromospheres. However, considering the discussion in the previous section, there is no reason to believe that, over a small range of T(eff) values, the generation of basal fluxes of acoustic power should give rise to dips of acoustic heating for stars that (i) lie within the range of T(eff) that is relevant to our sample, and (ii) have an amplitude as large as that which occurs in our Ca II flux data.

This leads us to revert to the possibility that acoustic power is not the sole contribution to chromospheric heating in our sample of stars. At first glance, this might seem surprising, since our sample is biased toward low-activity stars. But the presence of any finite magnetic field (whether generated by an $\alpha\Omega$ dynamo or by an α^2 dynamo or by an $\alpha^2\,\Omega$ dynamo) on a convective envelope will ensure that MHD waves are also generated. In H17, we have argued, based on RAC data, that the steeper RACs, which are observed in the high-activity stars with spectral types dK4e, dK6e, and dM2e stars, can be associated with the operation of an $\alpha\Omega$ dynamo in these stars. (Of course, the presence of an extensive convective envelope in all M dwarfs means that an α^2 dynamo can also be in operation.) The argument for an $\alpha\Omega$ dynamo in dK4e-dM2e stars is based on the fact that structural models of such stars (Stromgren 1952; Osterbrock 1953) indicate that an interface exists between a radiative core and the convective envelope. But in H17, we also argued that stars of high activity at later spectral types (dM3e, dM4e), do *not* have steep enough RACs to be considered sites of $\alpha\Omega$ dynamos. Instead, the overlap of the RAC slopes for the latest active stars with slopes of the RACs for inactive stars (dK4-dM4) led us to conclude that an α^2 dynamo (or perhaps an $\alpha^2\,\Omega$ dynamo; after all, the RAC does have a nonzero dependence on Ω) would be a better candidate to explain the RAC slopes in inactive stars *as well as in the latest (dM3e, dM4e) active stars*. Based on the data in H17, the effects of an $\alpha\Omega$ dynamo were hypothesized to "switch off" at a spectral type that lies between M2 and M3. In H17, the "switching off" of the operation of an $\alpha\Omega$ dynamo was presumed to be associated with TTCC. However, this transition is now known to be more complicated (Jao et al. 2018; MacDonald & Gizis 2018), so the conclusion of H17 needs to be re-stated in a more nuanced manner.

4.1. Distinguishing between Different Processes of Chromospheric Heating

When there is a possibility that more than one method of chromospheric heating may in principle be capable of operating in a star, the resulting heating of the chromosphere will, in general, not be expected to give rise to identical amounts of heating. Instead, if N methods are permissible, then method i will give rise to a level $F(i)$ of Ca II emission, where i varies from 1 to N. An important quantitative question arises: by how much might $F(i)$ differ quantitatively from $F(j)$? The range of possible answers can, in principle, be arbitrarily large. For the sake of simplicity, we consider here only the case $N = 3$, i.e., acoustic and two different magnetic components. Again, for simplicity, we assign one magnetic component to an $\alpha\Omega$ dynamo, and the other to an α^2 dynamo. Then we assume that the three components of heating lead to emission fluxes in (say) Ca II of $F(a)$, $F(\alpha\Omega)$, and $F(\alpha^2)$.

The values of $F(a)$ can be calculated with some confidence for a low-mass star with a specified effective temperature and gravity (see Section 3, where these fluxes were labeled by the notation F_A, in accordance with the notation used by Ulmschneider et al. 1996). However, the calculation of magnetic fluxes cannot be achieved with comparable confidence because of unknown parameters. The only thing that we can say with certainty about the magnetic fluxes ($F(\alpha\Omega)$ or $F(\alpha^2)$) is that both are nonnegative. For present purposes, we would like to determine if we can say anything plausible about the ratio of $F(\alpha\Omega)$ to $F(\alpha^2)$. In general, with different processes at work, $F(\alpha\Omega)$ and $F(\alpha^2)$ might differ from each other by significant factors.

In support of this conclusion, we may cite two different studies of dynamo properties. First, Durney et al. (1993) have reported on a model of an α^2-dynamo, i.e., one in which the magnetic field is generated by turbulent motions in the bulk of the solar convection zone (SCZ). In the presence of small-scale turbulence, when there exists an initial weak magnetic field, nonlinear transfer between magnetic field and velocity causes the magnetic energy on short length scales to build up as time progresses. Even in the absence of rotation, the magnetic energy on small scales (ME_S) eventually reaches a level almost as large as (within a factor of two) the equipartition value based on the kinetic energy on small scales (KE_s): in the presence of rotation, the approach to equipartition occurs on shorter timescales. On the other hand, there is also a build-up of magnetic energy on large scales (ME_L). However, Durney et al. find that the numerical value of ME_L turns out to be considerably smaller than ME_s. In the absence of rotation, the value of ME_L rises to only about $0.01ME_s$. Thus, this model predicts that turbulent convection leads preferentially to magnetic energy on *small* scales. Magnetic fields that are generated at the radiative convective interface depend on a different physical process: in this case, rotation plays an essential role. To describe the process, Durney et al. (1990) modeled a dynamo that they considered as closer to the solar cycle case. This dynamo lies near the base of the SCZ, where differential rotation contributes to an $\alpha\Omega$ dynamo. In this case, they found that the magnetic energy can grow to super-equipartition values. They referred to this as a "cycle field," because it helps to account for the 11 yr solar cycle. But Durney et al. (1990) stressed that "the SCZ could...generate a magnetic field with different properties than the cycle field," i.e., $F(\alpha\Omega)$ could differ from $F(\alpha^2)$. The sense of the difference was not mentioned by Durney et al. Second, Mason et al. (2002) have examined the properties of two dynamos in which the α-effect is concentrated (a) at the surface, and (b) near the base of the SCZ. They find that the dynamo is considerably more effective in case (b), i.e., when the α-effect is located close to the interface. Mason et al. conclude that an $\alpha\Omega$ dynamo operating near the base of the SCZ is "considerably more effective" than a surface α^2 dynamo. In this case, it seems likely that $F(\alpha\Omega)$ exceeds $F(\alpha^2)$.

Whatever the individual values of $F(a)$, $F(\alpha\Omega)$, and $F(\alpha^2)$ happen to be, the total amount of chromospheric emission flux that will be detected from any particular star is $F(\mathrm{tot}) = F(a) + F(\alpha\Omega) + F(\alpha^2)$. At any particular spectral type, we expect that $F(a)$ is always present at (more or less) the level that was quantified in Section 3. We can also assert that, since all the stars we study have deep convective envelopes, $F(\alpha^2)$ will be present to some extent in all of our stars at some level: what that level is in any particular star will probably depend most on how fast the star is rotating. Since this component is always present in late-type stars, it is possible that $F(\alpha^2)$ may contribute to the basal flux (in addition to acoustic power): this possibility is suggested by our findings in Section 3 above that acoustic power (as calculated by Ulmschneider et al. 1996) is not sufficient to account for *all* of the radiative losses in basal flux stars. And regarding $F(\alpha\Omega)$, we can say that it will be present in stars that are massive enough to have a radiative core, but it will be absent in completely convective stars.

Some information about the relative magnitude of $F(\alpha\Omega)$ and $F(\alpha^2)$ can be gleaned by considering stars belonging to a category in which both processes are potentially at work. We have already pointed out (see Figure 1 above), that inactive stars with spectral types dK4, dK6, and dM2 have RAC slopes that are definitely *shallower* than the RAC slopes for the active stars with the same spectral types (i.e., dK4e, dK6e, and dM2e stars). As in H17, we have interpreted the *steeper* dependence on rotation in the active stars as an indication that, in such stars, an $\alpha\Omega$ dynamo (with its greater sensitivity to rotation) is at work. On the other hand, the *shallower* slopes of the RAC in the inactive dK4, dK6, and dM2 stars is interpreted to mean that the dynamos in these stars are not as sensitive to rotation: specifically, we interpret the shallower slopes of the RAC as evidence that an $\alpha\Omega$ dynamo is *not* at work in the inactive dK4, dK6, and dM2 stars. Instead, since an α^2 dynamo is expected to be less sensitive to rotation, we believe that the shallow slopes of the RACs in the inactive stars can be interpreted to mean that an α^2 dynamo (or an $\alpha^2\,\Omega$ dynamo) is at work in those inactive stars.

When we examine the magnitudes of Ca II emission flux in active dKe and dMe stars at these types (where $F(\alpha\Omega) + F(\alpha^2)$ plus an acoustic component are present), and compare them to the fluxes in inactive dK and dM stars (where only $F(\alpha^2)$ plus an acoustic component are present), we find (using, e.g., Figures 2, 3, and 5 in H17) that the mean Ca II flux in the active stars exceeds that in the inactive stars by a factor of a few. This suggests that, at least in K4-M2 dwarfs, it could be permissible to conclude that $F(\alpha\Omega)$ exceeds $F(\alpha^2)$.

Let us hypothesize that at a certain spectral type, there is a transition from one magnetic mode to another: can we predict what we would see as we go to later spectral types? There are three possible outcomes: (a) the emission flux F(Ca II) increases; (b) F(Ca II) decreases; and (c) F(Ca II) stays the

same. If we are to make a theoretical choice between these possibilities, we need to have quantitative knowledge of the relative magnitudes of $F(\alpha\Omega)$ and $F(\alpha^2)$.

The scenario in which we are most interested here is the one in which $F(\alpha\Omega)$ maintains a nonzero value down to a spectral type that is as late as Mx where the radiative core disappears. On the one hand, stars that are slightly hotter than stars of spectral type Mx (we label such stars as having spectral type Mx-) are expected to have an overall flux in Ca II emission of $F(a) + F(\alpha\Omega) + F(\alpha^2)$. But because of the smallness of $F(a)$, this is essentially equal to $F(\alpha\Omega) + F(\alpha^2)$. On the other hand, stars that are slightly cooler than stars with spectral type Mx (we label such stars as having spectral type Mx+) will have an overall flux in Ca II emission of $F(a) + F(\alpha^2)$: once again, neglecting $F(a)$ due to its smallness, this is essentially equal to $F(\alpha^2)$. Now let us consider two limiting cases: (i) $F(\alpha\Omega) \ll F(\alpha^2)$, and (ii) $F(\alpha\Omega) \geqslant F(\alpha^2)$. In case (i), the disappearance of $F(\alpha\Omega)$ will have a negligible effect on F(tot) at spectral type Mx. In such a case, therefore, there would be *no reason* to expect to see any observational signature in the empirical flux of Ca II emission. It would indeed be unfortunate if we were unable to detect the location where $F(\alpha\Omega)$ disappears.

On the other hand, in case (ii), at spectral type Mx-, F(tot) will be essentially equal to $F(a) + F(\alpha\Omega)$, i.e., essentially $F(\alpha\Omega)$, whereas at Mx+, F(tot) will be equal to $F(a) + F(\alpha^2)$, i.e., essentially $F(\alpha^2)$. Therefore, F(tot) changes essentially from $F(\alpha\Omega)$ to $F(\alpha^2)$ when we pass through the transition from Mx- to Mx+. And since, by definition of case (ii), $F(\alpha\Omega)$ is $\geqslant F(\alpha^2)$, the emission flux in Ca II across the Mx transition will have the following signature: a clear step *downward*.

The numerical value of the ratio of the two flux totals at Mx- and Mx+ is expected to be $R(-+) = [F(a) + F(\alpha\Omega) + F(\alpha^2)]/[F(a) + F(\alpha^2)]$. Essentially, $R(-+)$ is equal to $1 + [F(\alpha\Omega)/F(\alpha^2)]$. If it happens that $F(\alpha\Omega) = F(\alpha^2)$, $R(-+)$ would be found to have a value of 2. If it happens that $F(\alpha\Omega) > F(\alpha^2)$, then $R(-+)$ would be found to have a value in excess of 2. Therefore, if case (ii) is applicable, the "step downward" in flux level is expected to be by a factor of 2 or more.

This is reminiscent of the "dip" that can be seen in Figure 3 above between spectral types M2.1 and M2.3: the step downward goes from a value of (about) 1.1 (on the y-axis) at M- to (about) 0.5 at M+, i.e., an amplitude of 2.2. Similar steps, with amplitudes that are also about 2, also occur in Figures 4 and 5 between the point labeled M1.8-M2.1 and the point labeled M2.2-M2.5. We suggest that the "dips" we have identified in Figures 3–5 may be a candidate for the "step downward" that was discussed above. If this interpretation is correct, we interpret the range of M2.1-M2.3 as an improved estimate of the transition between an $\alpha\Omega$ dynamo and an α^2 dynamo. In this context, the Ca II line fluxes at spectral type M2.1 (and earlier) have access to an $\alpha\Omega$ dynamo as well as an α^2 dynamo, whereas at spectral types M2.3 (and later), the stars can take advantage of only an α^2 dynamo.

5. Conclusion

In this paper, we have reported on an expanded data set of Ca II fluxes of chromospheric emission in a sample of roughly 600 M dwarfs. Our goal has been to determine if we can identify any signature in the chromospheric data that might be due to a transition from one form of dynamo operation to another. For example, TTCC, which is traditionally predicted to occur in stars with masses of order 0.3–0.35 $M_\odot$ on the lower main sequence, is expected to lead to the suppression of an interface dynamo: the disappearance of such a dynamo might reasonably be expected to be accompanied by an observational signature of some kind in the strength of chromospheric emission. In an earlier search for such a signature, using a smaller sample (less than 300 stars: H17), we focused on determining the numerical values of the *slope* of the RAC and used the slopes in search of a transition. Based on the behavior of the RAC slopes as a function of spectral type, H17 suggested that the switch in dynamo mode on the lower main sequence occurs at a spectral subtype between M2 and M3. To the extent that this dynamo switch is associated with the TTCC, H17 suggested that the TTCC lies between M2 and M3.

About a year after H17 was published, a completely independent study (based on *GAIA* photometry; Jao et al. 2018) reported that a structural change in stellar structure, leading to a dip in the luminosity function, makes its appearance "near spectral type M3.0V." Theoretical modeling (MacDonald & Gizis 2018) suggests that the *GAIA* dip is associated with complicated evolutionary effects as a star approaches the TTCC: the complications lead to the temporary appearance of a *small convective core* in low-mass stars in addition to the standard picture of radiative core plus outer convective envelope. It has long been known that dynamo activity in the Sun and stars is associated with the interface between radiative and convective regions. Now, the possibility of a new (inner) interface emerges with the existence of a small (temporary) convective core, separated from the outer convective envelope by a radiative region. The new inner interface may add an additional source of dynamo activity in low-mass stars. As a result, the dynamo mode may not undergo a transition solely at "the" (traditional) TTCC but also from the occurrence of a new dynamo mode deep in the interior.

With the expanded data set, we have, in this paper, examined the Ca II emission fluxes in greater detail. We have paid special attention to the range of spectral types from M1 to M3. We find that a "downward step" feature in this plot between spectral types M2.1 and M2.3 has properties that are consistent with the "switching off" of an important mode of chromospheric heating. We hypothesize that the mode of chromospheric heating that is switched off at the "step" is associated with an interface dynamo. We cannot say definitively whether the interface dynamo involved in the "downward step" lies at the inner or the outer interface, both of which are present during certain time intervals in the evolution of low-mass stars. If our hypothesis is correct, the new data suggest that the switch in dynamo mode may lie between M2.1 and M2.3. This range is consistent with, but more precise than, the conclusion of H17 that the switch in dynamo mode lies between M2 and M3. The new estimate of the location of the switch in dynamo mode corresponds to stars with T(eff) in the range 3610–3560 K.

We note that the location we have found for the switch in dynamo mode (M2.1-M2.3) is close to, but slightly earlier than, the spectral type "near M3.0V" that Jao et al. (2018) have reported as the location of an empirical dip in the luminosity function. MacDonald & Gizis (2018) have suggested that the dip seen by Jao et al. is associated with TTCC, which is known to occur in lower main-sequence stars (Limber 1958). Our data suggest that a switch in dynamo mode may occur at a spectral

type that is close to, but (if we take our results literally) somewhat earlier, than the TTCC. We suggest that the switch in dynamo mode that we suggest occurs at M2.1-M2.3 may be associated with the appearance of a small convective core. This gives rise to a new (inner) interface between radiative and convective gas in the deepest interior of the star (in addition to the well-known outer interface between radiative core and outer convective envelope). According to MacDonald & Gizis (2018), the dip seen by Jao et al. (2018) occurs at the time when the two convective regions (core and envelope) merge into a single convective zone extending from center to surface. MacDonald and Gizis have found that this merging process occurs sooner in lower-mass M dwarfs and later in more massive M stars: the merging occurs at an age of at least 9 b.y. in stars with mass 0.34 $M_{\odot}$, but at an age of less than 1 b.y. in stars with mass 0.31 $M_{\odot}$. In light of this difference in lifetimes, the inner interface dynamo is expected to survive longer in a more massive M dwarf, i.e., a star of earlier spectral type. This could bias the dynamo transition to somewhat earlier spectral types than the TTCC, perhaps explaining why we find M2.1-2.3 for the dynamo transition while the larger structural transition that appears in the luminosity function occurs at a slightly later spectral type, "near M3.0V" (Jao et al. 2018).

If we are correct in claiming that the presence of a second convective region (core) in an M dwarf may be associated with a switch in dynamo mode in such stars, then we need to consider that in other low-mass stars (including solar-like stars), a small convective core is also expected to be temporarily present. Could the presence of such a core lead to a signature of dynamo switching in solar-like stars also? We suggest two reasons why this is *not* likely to be detectable. First, in a solar-like star, the outer convective envelope remains so close to the surface (at radial locations of 0.7R(Sun) and larger) that there is little or no opportunity for a merger with the small convective core. Second, the relative values of two timescales are important: t(cc), the time interval during which the small convective core survives, and $t(s)$, the ages of the stars in our sample. As MacDonald & Gizis (2018) have shown, stars with masses corresponding to early M spectral type undergo merging of central core and convective envelope on timescales ranging from less than 1 Gyr to as long as 9 Gyr. Such time intervals are essentially identical with the (activity) ages of M dwarfs in the field (West et al. 2008: especially their Figure 10). Therefore, in our sample of 600 or so M dwarfs, it is highly likely that our stars include members with the correct age for merging of core and envelope. On the other hand, in a star with mass 1.0 M(Sun), J. MacDonald (2020, personal communication) reports that the convective core survives from age 29 Myr to age 102 Myr, i.e., much shorter than the ages associated with M dwarfs. In light of this result, in order to detect any observational signatures of dynamo switching that might be associated with such a core, we would have to examine activity data on solar-like stars with ages of 102 Myr and less. In a long-lasting observing program known as the *Sun in Time*, Guinan & Engle (2018) have reported on the coronal X-ray luminosity of solar-like stars (with spectral types G1.5V-G2.5V) with ages as old as 7 Gyr. For present purposes, we are especially interested in the *youngest* stars in the Guinan and Engle sample: they turn out to be members of the Pleiades, which has an age of 130 Myr (Bell et al. 2012). Thus, the data that are currently available for solar-like stars does *not* extend to ages that are young enough to overlap with the existence of a convective core. As a result, we do not yet have observations that would enable us to test whether or not an observational signature is present in the activity data related to the presence or absence of a small convective core.

We thank the referee for the extensive and constructive reports that have helped to sharpen the arguments in this paper. D.J.M. thanks Dr. J. MacDonald for a very helpful discussion of work on the inner convective core, including numerical values for the duration of such a core in the Sun, as well as for providing an estimate of $T_{\rm eff}$ for stars near the TTCC.

ORCID iDs

D. J. Mullan https://orcid.org/0000-0002-7087-9167
E. R. Houdebine https://orcid.org/0000-0002-0403-7519

References

Bell, C. P. M., Naylor, T., Maybe, N. J., Jeffries, R. D., & Littlefair, S. P. 2012, MNRAS, 424, 3178
Benevolenskaya, E. E. 1995, SoPh, 161, 1
Benevolenskaya, E. E. 1998, ApJL, 509, L49
Brandenburg, A. 2005, ApJ, 625, 539
Castellani, V., Puppi, I., & Renzini, A. 1971, Ap&SS, 10, 136
Charbonneau, P. 2014, ARA&A, 52, 251
Cram, L. E., & Giampapa, M. S. 1987, ApJ, 323, 316
Cram, L. E., & Mullan, D. J. 1979, ApJ, 234, 579
Cranmer, S. R., & van Ballegooijen, A. A. 2005, ApJS, 156, 265
Demircan, O., & Kahraman, G. 1991, Ap&SS, 181, 313
Doyle, J. G., Houdebine, E. R., Mathioudakis, M., & Panagi, P. 1994, A&A, 285, 233
Durney, B. R., De Young, D. S., & Passot, T. P. 1990, ApJ, 362, 702
Durney, B. R., De Young, D. S., & Roxburgh, I. W. 1993, SoPh, 145, 207
Fawzy, D. E., & Stepien, K. 2018, Ap&SS, 363, 57
Goodman, M. L. 1995, ApJ, 443, 450
Guinan, E. F., & Engle, S. G. 2018, RNAAS, 2, 12
Hammer, R., & Ulmschneider, P. 2007, in AIP Conf. Proc. 919, Kodai School of Solar Physics, ed. S. S. Hasan & D. Banerjee (Melville, NY: AIP), 138
Houdebine, E. R. 2010, MNRAS, 403, 2157
Houdebine, E. R., & Stempels, H. C. 1997, A&A, 326, 1143
Houdebine, E. R., Mullan, D. J., Bercu, B., Paletou, F., & Gebran, M. 2017, ApJ, 837, 96, H17
Houdebine, E. R., Mullan, D. J., Doyle, J. G., et al. 2019, AJ, 158, 56
Jao, W.-C., Henry, T. J., Gies, D. R., & Hambly, N. C. 2018, ApJL, 861, L11
Jess, D. B., Mathioudakis, M., & Keys, P. H. 2014, ApJ, 795, 172
Kuznetsov, M. K., del Burgo, C., Pavlenko, Yu. V., & Frith, J. 2019, ApJ, 878, 134
Leggett, S. K. 1992, ApJS, 82, 351
Lighthill, M. J. 1952, Proc. Roy. Soc, A211, 564
Limber, D. N. 1958, ApJ, 127, 387
Luhman, K. L., Stauffer, J. R., Muench, A. A., et al. 2003, ApJ, 593, 1093
MacDonald, J., & Gizis, J. 2018, MNRAS, 480, 1711
Mason, J., Hughes, D. W., & Tobias, S. M. 2002, ApJL, 580, L89
Mathioudakis, M., & Doyle, J. G. 1992, A&A, 262, 523
Morin, J. 2012, in Low Mass Stars and the Transition Stars/Brown Dwarfs, EES2011, ed. C. Reyle et al., Vol. 57 (Les Ulis: EDP Sciences), 165
Mullan, D. J. 1971, MNRAS, 154, 467
Mullan, D. J. 2009, Physics of the Sun: A First Course (Boca Raton, FL: CRC Press), 186
Mullan, D. J., & Cheng, Q. Q. 1993, ApJ, 412, 312
Mullan, D. J., Houdebine, E. R., & MacDonald, J. 2015, ApJL, 810, L18
Mursula, K., Ziegler, B., & Vilppola, J. H. 2003, SoPh, 212, 201
Musielak, Z. E., & Ulmschneider, P. 2002, A&A, 386, 606
Osterbrock, D. E. 1953, ApJ, 118, 529
Osterbrock, D. E. 1961, ApJ, 134, 347
Parker, E. N. 1955, ApJ, 122, 293
Parker, E. N. 1979, Cosmical Magnetic Fields (Oxford, UK: Clarendon Press)
Parker, E. N. 1988, ApJ, 330, 474
Paudel, R. R., Gizis, J. E., Mullan, D. J., et al. 2018, ApJ, 858, 55
Proudman, I. 1952, Proc Roy Soc, 214, 119

Racine, E., Charbonneau, P., Ghizaru, G., Bouchat, A., & Smolarkiewicz, P. K. 2011, ApJ, 735, 46
Rammacher, W., & Ulmschneider, P. 2003, ApJ, 589, 988
Reinhold, T., Cameron, R. H., & Gizon, L. 2017, A&A, 603, A52
Rutten, R. G. M., Schrijver, C. J., Lemmens, A. F. P., & Zwaan, C. 1991, A&A, 252, 203
Schrijver, C. J. 1983, A&A, 127, 289
Schrijver, C. J. 1987, A&A, 172, 111
See, V., Jardine, M., Vidotto, et al. 2016, in What can we Learn About Stellar Activity Cycles from ZDI? Zenodo, doi:10.5281/zenodo.156542
Spiegel, E. A., & Zahn, J.-P. 1992, A&A, 265, 106
Stauffer, J. R., & Hartmann, L. W. 1986, ApJS, 61, 531
Stenflo, J. O. 1991, in Lecture Notes in Physics, Vol. 380, The Sun and Cool Stars: Activity, Magnetism, Dynamos, ed. I. Tuominen et al. (Berlin: Springer), 193
Stromgren, B. 1952, AJ, 57, 65
Suarez Mascareno, A., Rebolo, R., & Gonzalez Hernandez, J. I. 2016, A&A, 595, A12
Ulmschneider, P., Rammacher, W., Musielak, Z. E., & Kalkofen, W. 2005, ApJL, 631, L155
Ulmschneider, P., Theurer, J., & Musielak, Z. E. 1996, A&A, 315, 212
Van Saders, J. L., & Pinsonneault, M. H. 2012, ApJ, 751, 98
West, A. A., Hawley, S. L., Bochanski, J. J., et al. 2008, AJ, 135, 785
Withbroe, G. L., & Noyes, R. W. 1977, ARA&A, 15, 363